THE JOURNAL OF BIOLOGICAL CHEMISTRY VOL. 286, NO. 22, pp. 19840–19859, June 3, 2011

Transcriptional Regulation of Pro-apoptotic Protein Kinase Cδ

IMPLICATIONS FOR OXIDATIVE STRESS-INDUCED NEURONAL CELL DEATH[*S]

Received for publication, November 15, 2010, and in revised form, March 28, 2011 Published, JBC Papers in Press, April 5, 2011, DOI 10.1074/jbc.M110.203687

Huajun Jin[‡], Arthi Kanthasamy[‡], Vellareddy Anantharam[‡], Ajay Rana[§¶], and Anumantha G. Kanthasamy[‡1]

From the [‡]Parkinson's Disorder Research Laboratory, Iowa Center for Advanced Neurotoxicology, Department of Biomedical Sciences, Iowa State University, Ames, Iowa 50011, the [§]Department of Pharmacology, Stritch School of Medicine, Loyola University Chicago, Maywood, Illinois 60153, and [¶]Hines VA Medical Center, Hines, Illinois 60141

We previously demonstrated that protein kinase Cδ (PKCδ; PKC delta) is an oxidative stress-sensitive kinase that plays a causal role in apoptotic cell death in neuronal cells. Although PKCδ activation has been extensively studied, relatively little is known about the molecular mechanisms controlling PKCδ expression. To characterize the regulation of PKCδ expression, we cloned an ~2-kbp 5′-promoter segment of the mouse *Prkcd* gene. Deletion analysis indicated that the noncoding exon 1 region contained multiple Sp sites, including four GC boxes and one CACCC box, which directed the highest levels of transcription in neuronal cells. In addition, an upstream regulatory region containing adjacent repressive and anti-repressive elements with opposing regulatory activities was identified within the region −712 to −560. Detailed mutagenesis studies revealed that each Sp site made a positive contribution to PKCδ promoter expression. Overexpression of Sp family proteins markedly stimulated PKCδ promoter activity without any synergistic transactivating effect. Furthermore, experiments in Sp-deficient SL2 cells indicated long isoform Sp3 as the essential activator of PKCδ transcription. Importantly, both PKCδ promoter activity and endogenous PKCδ expression in NIE115 cells and primary striatal cultures were inhibited by mithramycin A. The results from chromatin immunoprecipitation and gel shift assays further confirmed the functional binding of Sp proteins to the PKCδ promoter. Additionally, we demonstrated that overexpression of p300 or CREB-binding protein increases the PKCδ promoter activity. This stimulatory effect requires intact Sp-binding sites and is independent of p300 histone acetyltransferase activity. Finally, modulation of Sp transcriptional activity or protein level profoundly altered the cell death induced by oxidative insult, demonstrating the functional significance of Sp-dependent PKCδ gene expression. Collectively, our findings may have implications for development of new translational strategies against oxidative damage.

PKC represents a large family of at least 12 serine/threonine kinases that participate in a wide variety of cellular events, including proliferation, cell cycle progression, differentiation, and apoptosis (1). Based on their structure and substrate requirements, PKC isoforms are divided into the following three groups: conventional PKCs (α, βI, βII, and γ), novel PKCs (δ, ϵ, η, and θ), and atypical PKCs (ζ and ι/λ). As a novel PKC, PKCδ has been recognized as a key pro-apoptotic effector in various cell types (2, 3). The role of PKCδ in nervous system function is beginning to emerge, and recent studies show that PKCδ plays a role in regulation of receptor and channel activity, differentiation, migration, and apoptosis (4). In addition to lipid-mediated activation and phosphorylation activation, a new pathway of PKCδ activation, proteolytic cleavage, was discovered recently. Previously, we showed that PKCδ is an oxidative stress-sensitive kinase and that persistent activation of PKCδ by caspase-3-mediated proteolytic cleavage is a key mediator in oxidative stress-induced dopaminergic neurodegeneration (5–9). Alternatively, pharmacological inhibition of PKCδ and depletion of PKCδ by siRNA are each sufficient to prevent dopaminergic neurodegeneration in cell culture and animal models of Parkinson disease (10–12). We also showed that PKCδ negatively regulates tyrosine hydroxylase activity and dopamine synthesis by enhancing protein phosphatase 2A activity in dopaminergic neurons (13). An elevated striatal dopamine level was observed in PKCδ knock-out mice as compared with wild-type mice, further demonstrating a key role of the kinase in the nigrostriatal dopaminergic function (13). In addition, increased PKCδ activity, caused by aberrant expression of PKCδ, has been implicated in disease conditions, such as ischemia/hypoxia (14–17) and cancer (18–28). Therefore, an understanding of the molecular mechanisms that control the amount and activity of PKCδ is of physiological and pathophysiological interest.

PKCδ is ubiquitously expressed although the expression pattern is varied and complex (29–32). Evidence suggests that diverse stimuli can induce PKCδ expression (33–35, 37–39), but the detailed mechanisms responsible for transcriptional regulation of PKCδ, especially in neuronal cells, have never been explored. The PKCδ promoter is surprisingly complex and does not contain a TATA box. The considerably long 5′-untranslated region, as long as 675 bp in rat, is rarely found among the PKC family (40, 41). Moreover, a huge distance, nearly 17 kb in human and 12 kb in rat and mouse, is revealed between the transcription start and translation start sites (40, 41). To our knowledge, only a few studies have documented the

* This work was supported, in whole or in part, by National Institutes of Health Grants ES10586 (to A. G. K.), NS065167 (to A. K.), and GM055835 (to A. R.).

[S] The on-line version of this article (available at http://www.jbc.org) contains supplemental "Experimental Procedures," Figs. S1 and S2, Tables S1 and S2, and an additional reference.

The nucleotide sequence(s) reported in this paper has been submitted to the GenBank™/EBI Data Bank with accession number(s)GU182370.

[1] Holds the W. Eugene and Linda Lloyd Endowed Chair and Professorship. To whom correspondence should be addressed: Dept. of Biomedical Sciences, Iowa State University, 2062 College of Veterinary Medicine Building, Ames, IA 50011. Tel.: 515-294-2516; Fax: 515-294-2315; E-mail: akanthas@iastate.edu.

functional elements in the PKCδ promoter or the characteristics of the factors involved in the control of PKCδ transcription (42–45). In this study, we analyzed the mouse PKCδ promoter to identify the transcriptional mechanisms underlying neuronal PKCδ expression. By combining cell biological and molecular and biochemical approaches, we cloned ~2 kb of mouse PKCδ promoter, characterized multiple DNA regulatory elements that positively or negatively regulate PKCδ gene expression, and identified members of the Sp protein family of transcription factors, particularly the long Sp3 isoform, as fundamentally critical determinants of basal PKCδ gene transactivation. Furthermore, we also report that manipulation of PKCδ transcription through pharmacological inhibition of Sp transactivation or expression of a dominant-negative Sp3 effectively afforded an increased resistance to oxidative stress damage.

EXPERIMENTAL PROCEDURES

Reagents—Mithramycin A (MA)[2] and hydrogen peroxide (H_2O_2) were purchased from Sigma. Antibodies against PKCδ, phospho-PKCδ (Thr^{507}), Sp1, Sp3, and Sp4 were purchased from Santa Cruz Biotechnology (Santa Cruz, CA). SYTOX® Green fluorescent dye, Lipofectamine 2000 reagent, and all cell culture reagents were obtained from Invitrogen. Acetyl-DEVD-amino-4-methylcoumarin was obtained from Bachem (King of Prussia, PA).

Cloning of the 5′-Flanking Region of Prkcd Gene and Plasmid Construction—The 2.0-kb (−1694/+289) mouse PKCδ promoter sequence was amplified by fusion PCR from mouse genomic DNA prepared from the MN9D cells. Briefly, the −1694/−1193 and −1217/+289 fragments of the mouse PKCδ promoter first were amplified using mouse genomic DNA as a template and the primer sets P−1694F/P−1193R1 and P−1217F/P+289R (for all primers see supplemental Table S1), respectively. The two gel-purified PCR products then were mixed and used as a template to amplify the −1694/+289 fragment with the primer set P−1694F/P+289R. The conditions used in this second PCR were as follows: 95 °C for 2 min; 25 cycles of 95 °C for 45 s, 57.5 °C for 30 s, and 68 °C for 2 min; and 68 °C for 5 min. The resultant 2.0-kb PKCδ promoter fragment was inserted into XhoI/HindIII sites of pGL3-Basic luciferase vector (Promega, Madison, WI) and designated as pGL3−1694/+289. Using pGL3−1694/+289 as a template, a series of truncated PKCδ promoter reporter constructs were constructed by PCR with appropriate primers and cloned into pGL3-Basic vectors, similar to the preparation of pGL3−1694/+289. To generate the reporter plasmid pGL3−promoter−660/−561, fragment −660/−561 was PCR-amplified and inserted into the upstream of the SV40 promoter in pGL3−promoter vector (Promega). For construction of pGL3−660/−561 plus +2/+289, primer pairs P−660F/P−561+2R and P−561+2F/P+289R were used for application of fragments −660/−561 and +2/+289, respectively. The fusion fragment −660/−561 plus +2/+289 was then amplified by the fusion PCR technique as described above using the primers P−660F/P+289R, followed by cloning into pGL3-Basic vector. To generate plasmids pGL3−147/+2 plus +2/+289 or pGL3−147/+2 plus +289/+2, fragment +2/+289 was PCR-amplified using a primer pair P+2F/P+289R that included a flanking XhoI site at both ends, digested with XhoI, and cloned in either orientation into the pGL3−147/+2 reporter construct at the distant SalI site downstream of the luciferase gene. All reporter constructs were verified by DNA sequencing.

The expression plasmid bearing the cDNA of GFP-PKCδ was a kind gift from Dr. Mary Reyland, University of Colorado Health Sciences Center (Denver), and the pEGFP-C1 control vector was purchased from Clontech. The constructs for mammalian expression of pN3-Sp1, pN3-Sp4, and pN3-Sp3 FL encoding both long and short isoforms of Sp3 (46), the *Drosophila* actin promoter-driven expression vectors for Sp1 (pPac-Sp1), the short isoforms of Sp3 (pPac-Sp3), the long isoforms of Sp3 (pPac-USp3), the full length of Sp3 (pPac-Sp3 FL, which is equivalent to the mammalian vector pN3-Sp3FL), Sp4 (pPac-Sp4), and β-galactosidase (p97b) (47), and the "empty" control vectors pN3 and pPac0 were generously provided by Dr. G. Suske (Philipps-Universität Marburg, Germany). The plasmid pPac-Sp2 (48) was a kind gift from Dr. Dieter Saur (Technische Universität München, Germany). The p300 wild-type expression plasmid pCI-p300 and its histone acetyltransferase (HAT) deletion mutant, pCI-p300ΔHAT, were kindly provided by Dr. Joan Boyes (Institute of Cancer Research, UK) and generated as described previously (49). The empty vector pCIneo was a gift from Dr. Christian Seiser (University of Vienna, Austria). The expression plasmid pcDNA-CBP (50) was a gift from Dr. Xiang-Jiao Yang (McGill University, Canada). To generate the expression vector for dominant-negative form of Sp3 (amino acid 540–781), pN3-DN-Sp3 (51), the appropriated cDNA fragment was PCR-generated from pN3-Sp3 with the following primer pair: forward, 5′-ATATATCTCGAGACCATGGAGAATGCTGACAGTCCTG-3′ and reverse, 5′-ATATATAAGCTTTCAATGGTGATGGTGATGATGCTCCATTGTCTCATTTCC-3′. The PCR product was then subcloned into the pN3 vector. To generate the luciferase-reporter plasmids, Sp1-Luc and mSp1-Luc (51), which contains three consensus Sp1-binding sites underlined from SV40 promoter and three mutant Sp1-binding sites, respectively, the oligonucleotides with the sequences (Sp1-Luc, 5′-ATATATCTCGAGCGCGTGGGCGGAACTGGGCGGAGTTAGGGGCGGGAAAGCTTATATAT-3′; mSp1-Luc, 5′-ATATATCTCGAGCGCGTGTTTTGAACTGTTTTGAGTTAGGTTTTGGAAAGCTTATATAT-3′) were synthesized, annealed, and subcloned into the pGL3-Basic luciferase vector. To build the eukaryotic expression plasmid pcDNA-Sp2, Sp2 cDNA was cut out with XhoI from the pPac-Sp2 construct and inserted into the XhoI site of the pcDNA3.1 vector (Invitrogen).

Site-directed Mutagenesis—Point mutations of potential transcription elements (GC and CACCC motifs) were introduced into the proximal PKCδ promoter reporter plasmid pGL3−147/+289, pGL3−147/+209, or pGL3+165/+289 by using the GeneTailor site-directed mutagenesis system

[2] The abbreviations used are: MA, mithramycin A; HAT, histone acetyltransferase; H_2O_2, hydrogen peroxide; TFBS, transcription factor-binding sites; TSS, transcription start site; NRE, negative regulatory element; PKCδ, protein kinase Cδ; PD, Parkinson disease; CBP, cAMP-response element-binding protein-binding protein.

(Invitrogen) with overlapping PCR primers as indicated in supplemental Table S1, according to the manufacturer's instructions. To generate double mutants, plasmids carrying a single mutation were used as a template to further introduce the second mutation. For triple mutants, plasmids carrying double mutations were utilized. The mutated sequences of all mutants were confirmed by DNA sequencing.

Primary Mouse Striatal Neuronal Culture and Treatment—Plates (6-well) were coated overnight with 0.1 mg/ml poly-D-lysine. Striatal tissue was dissected from gestational 16–18-day-old murine embryos and kept in ice-cold Ca^{2+}-free Hanks' balanced salt solution. Cells then were dissociated in Hanks' balanced salt solution containing trypsin, 0.25% EDTA for 30 min at 37 °C. After enzyme inhibition with 10% heat-inactivated fetal bovine serum (FBS) in Dulbecco's modified Eagle's medium, the cells were suspended in Neurobasal medium supplemented with 2% Neurobasal supplement (B27), 500 μM L-glutamine, 100 units penicillin, and 100 units streptomycin, plated at 2×10^6 cells in 2 ml/well, and incubated in a humidified CO_2 incubator (5% CO_2 and 37 °C). Half of the culture medium was replaced every 2 days, and experiments were conducted using cultures between 6 and 7 days old. After exposure to doses of mithramycin A ranging from 0.5 to 5 μM for 24 h, the primary striatal cultures were subjected to quantitative real time RT-PCR or immunocytochemical analysis.

Cell Lines, Transient Transfections, and Reporter Gene Assays—The mouse dopaminergic MN9D cell line was a generous gift from Dr. Syed Ali (National Center for Toxicological Research/Food and Drug Administration, Jefferson, AR). The mouse neuroblastoma NIE115 cell line was a kind gift from Dr. Debomoy Lahiri (Indiana University School of Medicine, Indianapolis). The *Drosophila* SL2 cell line was purchased from ATCC (Manassas, VA). NIE115 and MN9D cells were cultured in Dulbecco's modified Eagle's medium supplemented with 10% FBS, 2 mM L-glutamine, 50 units of penicillin, and 50 units of streptomycin (37 °C, 5% CO_2). For H_2O_2 treatment studies, before addition of H_2O_2 (final concentration 0.5–2.0 mM), MN9D cells were switched to serum-free Dulbecco's modified Eagle's medium supplemented with 1× B27 supplement. *Drosophila* SL2 cells were maintained at 23 °C without CO_2 in Schneider's *Drosophila* medium containing 10% FBS.

Transient transfections of NIE115 and MN9D cells were performed using Lipofectamine 2000 reagent according to the manufacturers' instructions. Cells were plated at 0.3×10^6 cells/well in 6-well plates 1 day before transfection. Each transfection was performed with 4 μg of reporter constructs along with 0.5 μg of pcDNA3.1-βgal (Invitrogen) used to monitor transfection efficiencies. Cells were harvested at 24 h post-transfection, lysed in 200 μl of reporter lysis buffer (Promega), and assayed for luciferase activity. For cotransfection assays, various amounts of expression plasmids as indicated in figures were added to the reporter plasmids. The total amount of DNA was adjusted by adding an empty vector. In some experiments, mithramycin A (0–5 μM) was added 4 h after DNA transfection, and luciferase activity was measured 24 h later. For transfection of SL2 cells, 1 day before transfection, cells were plated onto 6-well plates at a density of 2.1×10^6 cells/well. Cells were transfected using the calcium phosphate transfection kit (Invitrogen), as described previously (52). Each well received 4 μg of reporter construct, 4 μg of β-galactosidase expression plasmid p97b for normalization of transfection efficiencies, and varying amounts (0–4 μg) of the fly Sp expression plasmids. DNA amounts of expression plasmids were compensated with the empty plasmid pPac0. After 24 h of transfection, the medium was changed, and 24 h later the cells were harvested, lysed by freeze-thawing in 200 μl of 0.25 M Tris-HCl (pH 7.8), and assayed for luciferase activity.

Luciferase activity was measured on a Synergy 2 MultiMode Microplate Reader (BioTek, Winooski, VT) using the luciferase assay system (Promega), and β-galactosidase activity was detected using the β-galactosidase enzyme assay system (Promega). The ratio of luciferase activity to β-galactosidase activity was used as a measure of normalized luciferase activity.

Quantitative Real Time RT-PCR—Total RNA was isolated from fresh cell pellets using the Absolutely RNA miniprep kit (Stratagene, La Jolla, CA). First strand cDNA was synthesized using an Affinity Script quantitative PCR cDNA synthesis kit (Stratagene). Real time PCR was performed in an Mx3000P quantitative PCR system (Stratagene) using the Brilliant SYBR Green quantitative PCR master mix kit (Stratagene), with cDNAs corresponding to 150 ng of total RNA, 12.5 μl of 2 × master mix, 0.375 μl of reference dye, and 0.2 μM of each primer in a 25-μl final reaction volume. All reactions were performed in triplicate. Sequences for PKCδ primers are shown in supplemental Table S1. β-Actin was used as internal standard with the primer set purchased from Qiagen (QuantiTect Primers, catalog number QT01136772). The PCR cycling conditions contained an initial denaturation at 95 °C for 10 min, followed by 40 cycles of denaturation at 95 °C for 30 s, annealing at 60 °C for 30 s, and extension at 72 °C for 30 s. Fluorescence was detected during the annealing step of each cycle. Dissociation curves were run to verify the singularity of the PCR product. The data were analyzed using the comparative threshold cycle (*Ct*) method (53).

Immunostaining and Microscopy—Immunostaining of PKCδ was performed in primary striatal neurons. Cells grown on coverslips pre-coated with poly-D-lysine were washed with PBS and fixed in 4% paraformaldehyde for 30 min. After washing, the cells were permeabilized with 0.2% Triton X-100 in PBS, washed with PBS, and blocked with blocking agent (5% bovine serum albumin and 5% goat serum in PBS). Cells then were incubated with the antibody against PKCδ (1:1000, Santa Cruz Biotechnology) overnight. Fluorescently conjugated secondary antibody (Alexa 568-conjugated anti-rabbit antibody red, 1:1500) was used to visualize the protein. Nuclei were counterstained with Hoechst 33342 for 3 min at a final concentration of 10 μg/ml. Finally, images were viewed using an oil immersion 60× Plan Apo lens with a 1.45 numerical aperture on a Nikon inverted fluorescence microscope (model TE2000, Nikon, Tokyo, Japan). Images were captured with a SPOT color digital camera (Diagnostic Instruments, Sterling Heights, MI) and processed using Metamorph 5.07 image analysis software (Molecular Devices). For quantitative analysis of immunofluorescence, we measured average pixel intensities from the region of interest using the Metamorph 5.07 image analysis software.

Immunoblotting—Cell lysates were prepared as described previously (12). Immunoblotting was performed as described previously (12). Briefly, the samples containing equal amounts of protein were fractionated through a 7.5–15% SDS-PAGE and transferred onto a nitrocellulose membrane (Bio-Rad). Membranes were blotted with the appropriate primary antibody and developed with either IRDye 800 anti-rabbit or Alexa Fluor 680 anti-mouse secondary antibodies. The immunoblot imaging was performed with an Odyssey Infrared Imaging system (LI-COR, Lincoln, NE).

Nuclear Extract Preparations and EMSA—NIE115 nuclear extract was prepared as described previously (54). For EMSAs, the IRDye 700-labeled complementary single-stranded oligonucleotides corresponding to sequences +205 to +236 of the mouse PKCδ promoter were synthesized (LI-COR), annealed, and used as labeled probe. The unlabeled competitor oligonucleotides were obtained from Integrated DNA Technologies, Inc. (Coralville, IA). The sequences of oligonucleotides used for EMSAs are illustrated in supplemental Table S2. In each reaction, 50 fmol of labeled probes and 10 μg of nuclear extracts were added. The resulting DNA-protein complexes were resolved on a 7% nondenaturing polyacrylamide gel and analyzed on the Odyssey imaging system (LI-COR). In competition experiments, before the addition of the labeled probe, nuclear extracts were preincubated for 30 min at room temperature with a 100-fold molar excess of unlabeled competitor oligonucleotides.

Chromatin Immunoprecipitation (ChIP)—ChIP assays were conducted with chromatin isolated from NIE115 cells using the ChIP-IT Express enzymatic kit from Active Motif, according to the manufacturer's instructions with slight modifications. Briefly, after cross-linking, the nuclei were prepared and applied to enzymatic digestion to generate chromatin fragments between 200 and 1500 bp. The sheared chromatin was collected by centrifugation, and a 10-μl aliquot was removed to serve as a positive input sample. Aliquots of 70-μl sheared chromatin were immunoprecipitated with 3 μg indicated antibody and protein-G magnetic beads. Equal aliquots of each chromatin sample were saved for no-antibody controls. The immunoprecipitated DNA was analyzed by PCR using PKCδ-specific primer set P+2F/P+289R as indicated in supplemental Table S1 to amplify a region (+2 to +289) within the PKCδ promoter. Conditions of linear amplification were determined empirically for these primers. PCR conditions are as follows: 94 °C 3 min; 94 °C 30 s, 59 °C 30 s, and 68 °C 30 s for 35 cycles. PCR products were resolved by electrophoresis in a 1.2% agarose gel and visualized after ethidium bromide staining.

DNA Fragmentation Assays—DNA fragmentation assay was performed using a cell death detection ELISA Plus kit as described previously (5). Briefly, after treatment with various doses of H_2O_2 for 20 h, MN9D cells were collected and lysed in 450 μl of lysis buffer supplied with the kit for 30 min at room temperature and spun down at 2300 × *g* for 10 min to collect the supernatant. The supernatant then was used to measure DNA fragmentation as per the manufacturer's protocol. Measurements were made at 405 and 490 nm using a SpectraMax 190 spectrophotometer (Molecular Devices).

SYTOX® Green Cytotoxicity Assays—Cell death was determined after exposing the MN9D cells to H_2O_2 using the SYTOX® Green cytotoxicity assay, as described previously (7). SYTOX® Green dye is a vital probe of low background fluorescence that is excluded from cells with intact membranes, but it labels nucleic acids in cells that have impaired membrane integrity to produce green fluorescence (55, 56). In brief, after treatment with H_2O_2 (0.5–1 mM) for the indicated time periods, SYTOX® Green fluorescent dye (1 μM) was added and incubated for 1 h at 37 °C. The cytotoxic cell death was then quantified by measuring DNA-bound SYTOX® Green fluorescence using the Synergy 2 MultiMode Microplate Reader (excitation 485 nm; emission 538 nm). Also, fluorescent images of SYTOX-positive cells were taken with a Nikon TE2000 microscope, and pictures were captured with a SPOT digital camera.

Caspase-3 Enzymatic Assays—Caspase-3 activity was measured as described previously (57). Briefly, after treatment with 1 mM H_2O_2, MN9D cells were resuspended in caspase lysis buffer (50 mM Tris-HCl (pH 7.5), 1 mM EDTA, 10 mM EGTA, and 10 μM digitonin) at 37 °C for 20 min. Lysates were prepared by centrifuge and then incubated with a specific fluorescent substrate, Ac-DEVD-amino-4-methylcoumarin (50 μM), at 37 °C for 1 h. Caspase-3 activity was then measured using a SpectraMax Gemini XS Microplate Reader (Molecular Devices, Sunnyvale, CA) with excitation at 380 nm and emission at 460 nm. The caspase-3 activity was calculated as fluorescence units/mg of protein.

Bioinformatics—The search for phylogenetic sequence conservation among rat, human, and murine PKCδ promoter was conducted with the program DiAlign TF (Genomatix Software) (58). This program identifies common transcription factor-binding site (TFBS) matches located in aligned regions through a combination of alignment of input sequences using the program DiAlign with recognition of potential TFBS by MatInspector software (Genomatix Software) (59).

Statistical Analysis—Unless otherwise stated, all data were determined from three independent experiments, each done in triplicate, and expressed as average values ± S.E. All statistical analyses were performed using the GraphPad Prism 4.0 software (GraphPad Software, San Diego). One-way analysis of variance test followed by the Tukey multiple comparison test were used for statistical comparisons, and differences were considered significant if p values less than 0.05 were obtained.

RESULTS

Identification of DNA Elements Involved in Transcriptional Regulation of Mouse Prkcd Gene—The mouse *Prkcd* gene, located on mouse chromosome 14, includes 18 exons that span ~20 kb (Fig. 1*A*). The PKCδ promoter lacks a TATA box and contains GC-rich sequences in the proximal promoter region. Furthermore, examination of the PKCδ promoter did not reveal the classic initiator elements or the downstream promoter elements, which are located at various distances downstream of the transcription start site (TSS) and are utilized by most TATA-less promoters to initiate transcription, suggesting that there might be other promoter motifs involved in the regulation of PKCδ gene transcription. To facilitate analysis of the regulation of the PKCδ promoter, an ~2-kbp fragment containing the

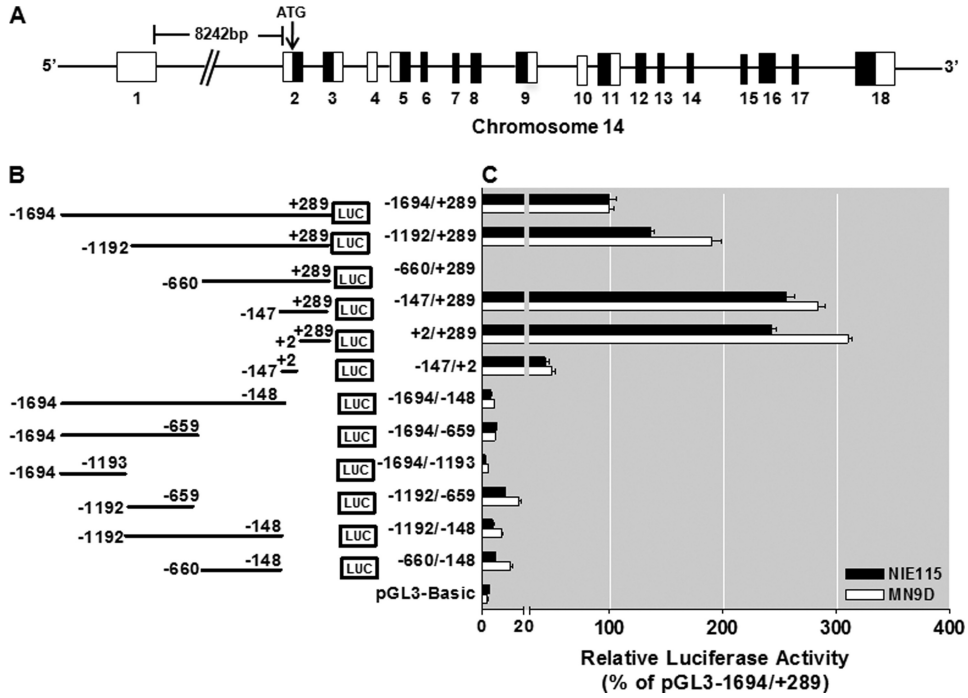

FIGURE 1. **Deletion analysis of PKCδ promoter activity in NIE115 and MN9D cells.** *A*, schematic diagram of mouse PKCδ gene structure on chromosome 14. Exons are marked by *boxes* and are numbered *below* each box, and *black* and *white* regions within the *boxes* indicate the coding and noncoding exons, respectively. *Arrow* indicates the position of the translation start codon (ATG). *B*, schematic representation of PKCδ promoter deletion/luciferase reporter constructs. An extensive series of PKCδ promoter deletion derivatives was generated by PCR methods and inserted into the pGL3-Basic luciferase vector. The 5′- and 3′-positions of the constructs with respect to the transcription start site are depicted. *C*, each construct as shown in *B* was transiently transfected into NIE115 (*black bar*) and MN9D (*white bar*) cells. Cells were harvested 24 h after transfection, and luciferase activities were determined. The plasmid pcDNA3.1-βgal was included in each transfection to normalize the promoter activity with transfection efficiency. The activity of full-length promoter construct (pGL3−1694/+289) was arbitrarily set to 100, and the relative luciferase activity of the other constructs was calculated accordingly. The results represent the mean ± S.E. of three independent experiments performed in triplicate.

putative PKCδ promoter (1694 bp), as well as partial sequences of the first, noncoding exon (289 bp), was amplified by the fusion PCR technique from MN9D cells. This sequence has been deposited in the GenBank™ under accession number GU182370. The resulting −1694/+289 region of the PKCδ promoter was placed upstream of the pGL3-Basic vector, designated as pGL3−1694/+289, and it was transiently transfected into NIE115 and MN9D cells along with the pcDNA3.1-βgal plasmid to monitor transfection efficiency. Luciferase activity of this construct increased nearly 30-fold as compared with the pGL3-Basic control, suggesting that this 2-kb sequence possesses functional promoter activity in both cells (Fig. 1, *B* and *C*). To further delineate the location of functional elements that govern the PKCδ promoter activity, we introduced a series of truncated promoter fragments in the pGL3−1694/+289 construct by PCR and cloned into the pGL3-Basic vector. Both NIE115 and MN9D cells displayed similar profiles of reporter activity upon transfection with these reporter constructs. Two constructs pGL3−147/+289 and pGL3+2/+289, which contain sequences with high GC content in the proximal first exon, each exhibited a maximal luciferase activity that averaged ~260% of the activity of the pGL3−1694/+289 construct in both cells. Furthermore, lack of the sequence from +2 to +289 led to near background reporter activity in six truncated promoter constructs (pGL3−1694/−148, pGL3−1694/−659, pGL3−1694/−1193, pGL3−1192/−659, pGL3−1192/−148, and pGL3−660/−148). Thus, these data suggest the particular importance of the GC-rich sequences in the region between +2 and +289 for sustaining PKCδ gene transcription in neuronal cells. It should be noted that a vector, pGL3−147/+2 containing the −147/+2 fragment in which the basal promoter region was placed to drive luciferase expression, demonstrated modest transcriptional activity (average activity in both cells, ~45% of that produced by the construct pGL3−1694/+289). Addition of the 5′-fragment of −660 to −147 into the pGL3−147/+289 construct resulted in a complete loss of activity in construct pGL3−660/+289, indicating the presence of a strong repressive element that negatively regulated transcription activity within the −660 to −147 region. Further addition of the 5′-sequence from −1192 to −660 into the pGL3−660/+289 construct partially blocked this repressive effect, indicating that the region (between 1192 and −660) contained either an enhancer element or an anti-repressor element that overcame the repression. Construct pGL3−1192/−660, however, displayed no luciferase activity in either cell line, and thus, within this region (−1192 to −660 bp) an anti-repressive element existed but not an enhancer element. The region between −1694 and −1193 may contain a weak inhibitory *cis*-element, as deletion of this ~500 bp from the construct pGL3−1694/+289 resulted in a slight increase in the promoter activity. Taken together, these results demonstrate that the PKCδ promoter contains multiple positive and negative regulatory elements in NIE115 and MN9D cells. The GC-rich region located between bp +2 and +289 contains a sequence of nucleotides necessary for transcription of the mouse *Prkcd* gene, and the sequence between

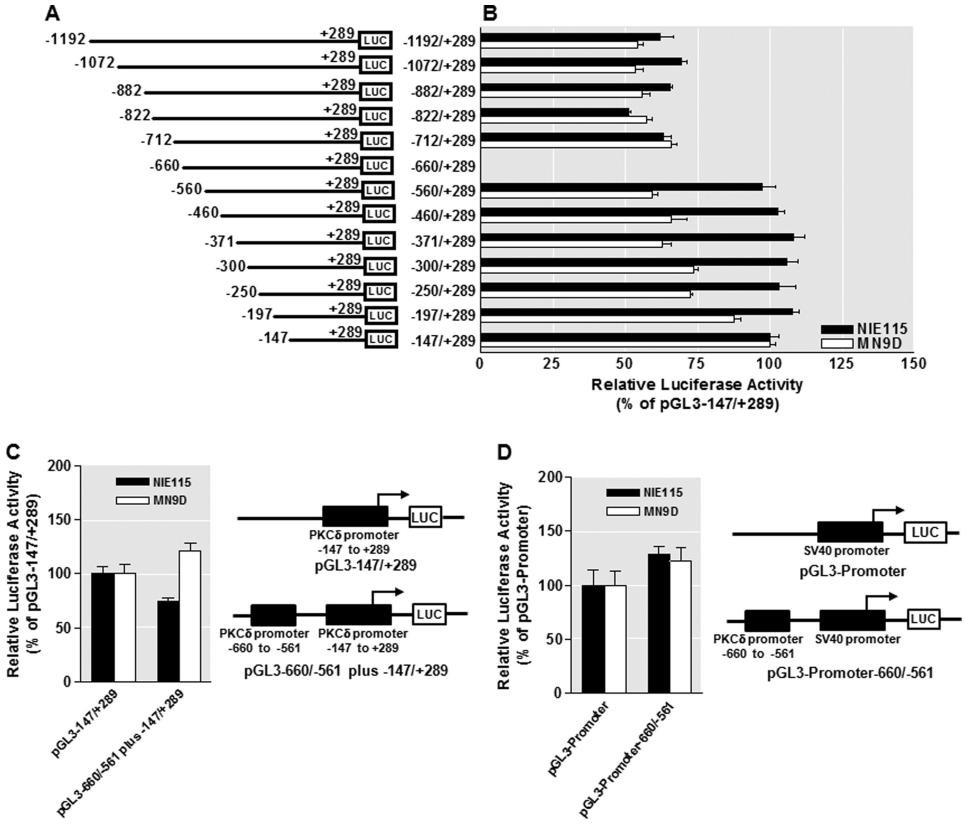

FIGURE 2. **Mapping of the identified repressive and anti-repressive elements within the PKCδ promoter and evidence for the PKCδ promoter-specific repressive element.** *A*, schematic representation of PKCδ promoter 5′-deletion constructs used for the fine mapping study. The 5′- and 3′-positions of the constructs with respect to the transcription start site are depicted. *B*, each construct as depicted in *A* was transiently transfected into NIE115 (*black bar*) and MN9D (*white bar*) cells. Cells were harvested 24 h after transfection for assaying luciferase activities. The plasmid pcDNA3.1-βgal was cotransfected into cells for data normalization. The activity of pGL3−147/+289 was arbitrarily set to 100, and the relative luciferase activity of the other constructs is presented. The results represent the mean ± S.E. of three independent experiments performed in triplicate. *C*, isolated repressive element of the PKCδ promoter does not function as a locus-independent DNA element. The sequences around the identified repressive element (−660 to −561 of the PKCδ promoter) were directly fused to the 5′-end of the region between −147 to +289 of the PKCδ promoter and cloned into the pGL3-Basic luciferase vector to obtain pGL3−660/−561 plus −147/+289. NIE115 (*black bar*) and MN9D cells (*white bar*) were transfected with pGL3−147/+289 or pGL3−660/−561 plus −147/+289 for 24 h, and luciferase activity was determined. Schematic diagram of these constructs are shown at the *right*. The activity of pGL3−147/+289 was set to 100, and the relative luciferase activity of pGL3−660/−561 plus −147/+289 is presented. The results represent the mean ± S.E. of three independent experiments performed in triplicate. *D*, isolated repressive element of the PKCδ promoter does not act on a heterologous promoter (SV40). The sequences of the putative PKCδ repressive element (−660 to −561 of the PKCδ promoter) were cloned upstream of the SV40 promoter in pGL3−promoter vector to obtain pGL3−promoter-660/−561. NIE115 (*black bar*) and MN9D (*white bar*) cells were transfected with pGL3−promoter or pGL3−promoter-660/−561 for 24 h, and luciferase activity was determined. Schematic diagram of these constructs are shown at the *right*. The activity of pGL3−promoter was set to 100, and the relative luciferase activity of pGL3−promoter-660/−561 is given. The results represent the mean ± S.E. of three independent experiments performed in triplicate.

−660 to −147 and 1192 to −660 contains a strong negative regulatory element (NREI) and an anti-repressive element with opposing activities controlling PKCδ gene expression. The region of −1694 to −1193 also contains a weak negative regulatory element (NREII).

Next, the identified negative regulatory element and anti-repressive element within the region between −1192 and −148 were investigated in more detail. First, to define the borders of these regulatory elements more precisely, series of detailed 5′-deletions were constructed in this region and tested for their relative transcriptional activity utilizing the −147/+289 fragment as the base line. As shown in Fig. 2, *A* and *B*, in either MN9D or NIE115 cells, the anti-inhibitory effect of the anti-repressive element was retained, even after deletion of the sequence between nucleotides −1192 and −712. However, the anti-inhibitory effect was completely abolished when the sequence between −712 and −660 was deleted, suggesting that the anti-repressive element resides between the nucleotides −712 and −660. Further deletion of the region between −660 and −560 restored almost full promoter activity; however, all six of the 5′-deletion constructs from −560 to −197 exhibited comparable transcriptional activities to that of the −147/+289 fragment. This suggests that the NREI is limited to the region between −660 and −560.

Two functional types of NRE have been defined as follows: promoter-specific NRE and the so-called silencer elements that are able to repress promoter activity in an orientation- and position-independent fashion, as well as in the context of both native and heterologous promoters (60). To further characterize the functional properties of the NREI in the PKCδ promoter, a chimeric fragment corresponding to the transcriptionally inhibited sequence from −660 to −561 was subcloned immediately 5′ of the PKCδ proximal promoter construct pGL3−147/+289 to obtain pGL3−660/−561 plus −147/+289. As shown in Fig. 2*C*, the repressive activity of this region was significantly attenuated, and indeed, the luciferase activity

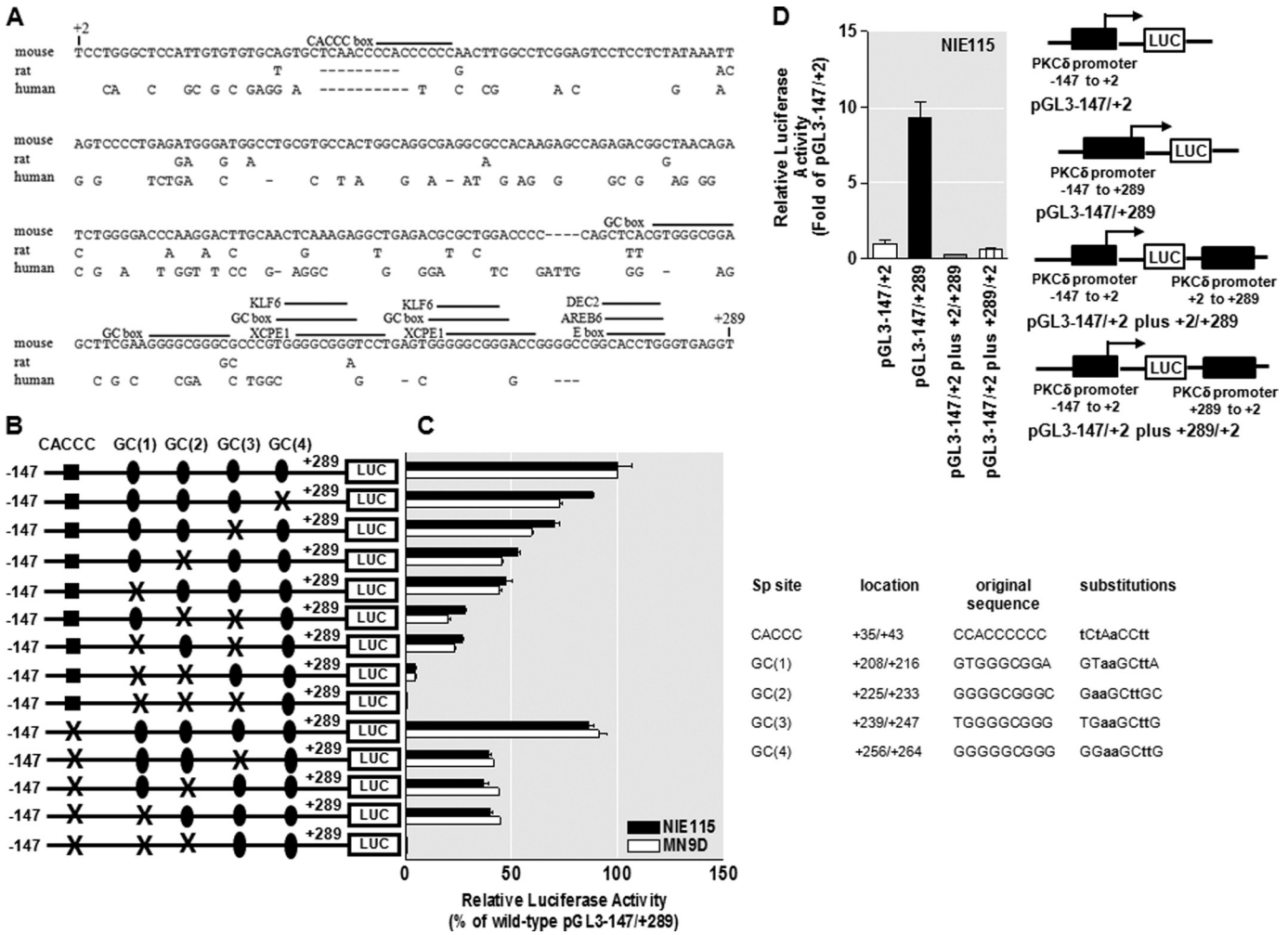

Sp site	location	original sequence	substitutions
CACCC	+35/+43	CCACCCCCC	tCtAaCCtt
GC(1)	+208/+216	GTGGGCGGA	GTaaGCttA
GC(2)	+225/+233	GGGGCGGGC	GaaGCttGC
GC(3)	+239/+247	TGGGGCGGG	TGaaGCttG
GC(4)	+256/+264	GGGGGCGGG	GGaaGCttG

FIGURE 3. **Functional analysis of the PKCδ proximal promoter.** *A*, sequence comparison of the mouse PKCδ promoter region between +2 to +289 with the corresponding regions of the rat and human PKCδ promoters. Sequences were aligned with the DiAlign TF program. Sequence differences are indicated, and gaps introduced to maximize homology are marked by *dashes*. Phylogenetically conserved TFBS as well as the CACCC box present only in the mouse PKCδ promoter are indicated (*overlined*). *B*, schematic representation of the wild-type or mutated PKCδ promoter reporter constructs containing targeted substitutions in the Sp-binding sites. The potential Sp sites are indicated at the *top*. The mutated site is marked with ×, and the nonmutated Sp sites are indicated by either *circle* or *square*. *C*, wild-type or mutated reporter constructs as shown in *B* were individually transfected into NIE115 (*black bar*) and MN9D (*white bar*) cells, and luciferase activities were assayed after 24 h. To adjust for transfection efficiency, the plasmid pcDNA3.1-βgal was included in each transfection. The activity of wild-type construct (pGL3−147/+289) was arbitrarily set to 100, and promoter activity of the mutants is expressed as a percentage of the wild-type construct. The results represent the mean ± S.E. of three independent experiments performed in triplicate. The sequences of wild-type and mutated Sp site are shown at the *right side* of the bar graph. The substituted nucleotides are shown in *boldface*. *D*, absence of enhancer elements in the GC-rich sequence (+2/+289) of the mouse PKCδ promoter in NIE115 cells. The PKCδ promoter GC-rich sequence (+2 to +289) was cloned in both orientations into the SalI site of the pGL3−147/+2 reporter constructs as described under "Experimental Procedures." These constructs were individually transfected into NIE115 cells for 24 h, and luciferase activity was determined. Luciferase activity was normalized with β-galactosidase. The *right panel* shows the schematic diagram of the constructs. The activity of pGL3−147/+2 was set to 1, and the relative luciferase activity of all other constructs were calculated and expressed as fold of pGL3−147/+2. The results represent the mean ± S.E. of three independent experiments performed in triplicate.

in MN9D cells was actually increased, suggesting that the inhibitory activity of this repressive element is dependent upon its physical location in the PKCδ promoter. Furthermore, when the same fragment was placed 5′ upstream of the heterologous SV40 early promoter (pGL3 promoter−660/−561, see Fig. 2*D*), no repressive activity was observed in either NIE115 or MN9D cells. Taken together, these data demonstrate that the NREI in the PKCδ promoter is functioning mechanistically as a promoter-specific repressive element but not as a classic transcriptional silencer element.

Five Sp Sites Act as Crucial cis-Elements Regulating the PKCδ Promoter—We further concentrated our studies on the sequences with high GC content between +2 and +289 because experiments described earlier suggested the critical role of this proximal 288-bp region in the regulation of mouse PKCδ transcription. A comparison of this region with the corresponding regions of the rat and human PKCδ genes using a DiAlign TF program (59) revealed that this region is conserved between all three species; the identities are 89, 60, and 61% between rat and mouse, human and mouse, and human and rat, respectively (Fig. 3*A*). Furthermore, the regions of all species are GC-rich and contain >66% GC content. Subsequent analysis with the program MatInspector (59) revealed the presence of a number of potentially important transcription factor-binding sites that are phylogenetically conserved among all species (identities are more than 95%), including four consecutive GC boxes (consensus GGGGCGGGG) designated GC(1) to GC(4) within ~250 bp downstream of the TSS. In addition, a CACCC

box (also called GT box) that matches consensus CCACCCC was found at position +35 bp downstream of the TSS (Fig. 3*A*). GC boxes, GT/CACCC box, and related GC-rich motifs, which are frequently designated Sp sites, often act as the binding sites for Sp transcription factors to regulate the basal and induced transcription of the core promoter as well as operate as essential enhancer sequences (61, 62). The functional importance of different Sp-binding sites for transactivation of the PKCδ promoter was investigated by site-directed mutagenesis of these binding sites within the context of the PKCδ reporter construct pGL3−147/+289. Transient transfections of NIE115 and MN9D cells were carried out with these mutant constructs, and promoter activity was determined and expressed relative to that of the wild-type construct. As shown in Fig. 3, *B* and *C*, the mutation of the CACCC box at +35 slightly diminished promoter activity in NIE115 (~15%) and MN9D (~10%) cell lines as compared with the wild-type construct. Alteration of the most distal GC(4) site at +256 displayed ~12 and 30% reduction in promoter activity over the wild-type construct in NIE115 and MN9D cells, respectively, whereas the inhibition observed with the GC(3) mutant, located just upstream of GC(4), was more pronounced, (reduced by ~30 and 40% in NIE115 and MN9D cells, respectively). In contrast, mutation of either the proximal GC(2) box or GC(1) box caused major decrements in reporter activity (~50 and 55% elimination in NIE115 and MN9D cells, respectively), suggesting that GC(2) and GC(1) represent more important motifs in activating the PKCδ promoter in comparison with the GC(3), GC(4), and CACCC sites. To investigate the regulatory interplay of different Sp sites, we performed simultaneous mutations of different Sp sites, and more reductions in promoter activity were seen with this strategy, thus suggesting that a functional synergism between these Sp sites is critical for the PKCδ promoter activity. For example, double mutations ablating the CACCC box with the GC(3) box, or GC(2) box, or GC(1) box resulted in a reduction of promoter activity by ~60% in both cell lines. However, double mutations of GC(3) and GC(2) boxes, or GC(3) and GC(1) boxes, reduced the activity of the PKCδ promoter in NIE115 and MN9D cells by ~73 and 80%, respectively. A further reduction in promoter activity by ~95% occurred when both the GC(2) box and GC(1) box were mutated. Finally, triple mutations of CACCC, GC(2), and GC(1) sites, or triple mutations of GC(3), GC(2), and GC(1) sites entirely abolished the PKCδ promoter activity. Taken together, these functional data suggest that GC(1) and GC(2) sites, and less significantly, GC(3), GC(4), and CACCC sites, are critical *cis*-elements for constitutive expression of PKCδ in neuronal cells. In addition, these Sp sites can cooperate in an additive manner to regulate the PKCδ promoter transactivation.

Given the great enhancing effect of the crucial GC-rich motif from +2 to +289 bp on the transcriptional activity of the PKCδ basal promoter region −147 to +2 (Fig. 1), we next investigated whether this GC-rich domain is sufficient to function as an enhancer element in NIE115 cells. To address this, the sequences around the region between +2 and +289 were subcloned in either orientation into the pGL3−147/+2 reporter construct, at the distant SalI site downstream of the luciferase stop codon (pGL3−147/+2 plus +2/+289 or pGL3−147/+2 plus +289/+2, see Fig. 3*D*). Then the relative transcriptional strength of these constructs was measured in NIE115 cells. The results showed that, somewhat surprisingly, the GC-rich motif in either orientation and at some distance completely lost the ability to enhance transcription compared with the vector pGL3−147/+289 (Fig. 3*D*). These data demonstrate that the GC-rich fragment is distance- and orientation-dependent, and thus it cannot operate as a classic enhancer element for PKCδ transcription in NIE115 cells.

PKCδ Promoter Expression Is Stimulated by Sp1, Sp2, Sp3, and Sp4 in NIE115 Cells and MN9D Cells—The Sp family members, including Sp1, Sp2, Sp3, and Sp4, are the major transcription factors that bind to the GC box, GT/CACCC box, and other closely related GC-rich motifs. Sp1, Sp2, and Sp3 are ubiquitously expressed in mammalian cells, whereas Sp4 expression is restricted to brain tissue (62). All of them share the same target sequences with similar binding affinities. To assess the functional significance of those Sp family proteins for the activity of mouse PKCδ promoter, various amounts (from 4 to 8 μg) of expression vectors for Sp1 (pN3-Sp1), Sp2 (pcDNA-Sp2), the full length of Sp3 (pN3-Sp3 FL encoding both long and short isoforms of Sp3), Sp4 (pN3-Sp4), and empty vectors (pN3 or pcDNA3.1) were individually cotransfected along with the PKCδ promoter construct pGL3−147/+289 into NIE115 and MN9D cells. Normalized luciferase activities were expressed as fold induction over cotransfections with empty vectors. As shown in Fig. 4*A*, all four Sp proteins exhibited a dose-dependent activation of PKCδ luciferase activity in NIE115 cells, with Sp3 being the most potent transactivator (1.4–2.3-, 1.2–1.6-, 1.4–3.1-, and 1.4–2.4-fold stimulation for Sp1, Sp2, Sp3, and Sp4, respectively). These results suggest that all Sp transcription factors can potently transactivate the PKCδ promoter in NIE115 cells. Likewise, overexpression of Sp3 in MN9D cells transactivated the PKCδ promoter in a dose-dependent manner from 1.5- to 2.5-fold. However, Sp1, Sp2, and Sp4 activated the PKCδ promoter much less efficiently than Sp3 in MN9D cells (maximal inductions of only 1.2-, 1.8-, and 1.2-fold with 8 μg of Sp1, Sp2, or Sp3 expression vector, respectively), suggesting that Sp3 is a strong activator of mouse PKCδ transcription in MN9D cells, whereas Sp1, Sp2, and Sp4 are weak. Overexpression of Sp1, Sp3, and Sp4 in transfected NIE115 (Fig. 4*B*, *left panel*) and MN9D (Fig. 4*B*, *right panel*) was verified by Western blot analysis. Note that Sp3 and Sp4 are endogenously expressed at appreciable levels in either cell line, but unexpectedly, the expression of endogenous Sp1 was not detected in both cells, which is discordant with the fact that Sp1 is a ubiquitous transcription factor.

Members of the Sp family share a high affinity to the same GC-rich binding sequences, and therefore they can act synergistically or antagonistically to activate transcription, depending on the nature of the cell and the promoter context. To investigate whether synergism or competition exists between these Sp family members to modulate expression of the PKCδ promoter, cotransfections of NIE115 were performed with various combinations of these Sp transcription factors, together with the PKCδ reporter construct pGL3−147/+289. As shown in Fig. 4*C*, coexpression of 4 μg of pN3-Sp1 and pN3-Sp3 FL expression vectors stimulated PKCδ promoter transcription by

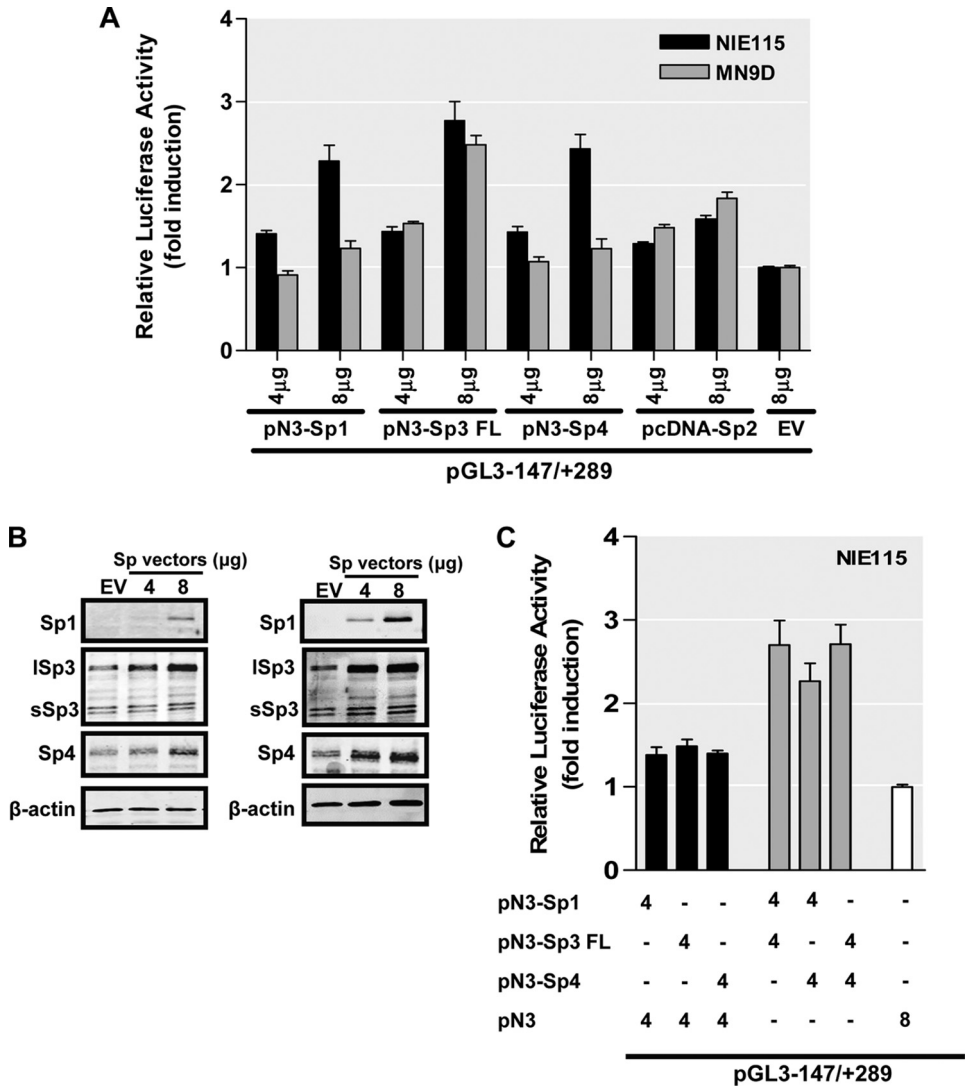

FIGURE 4. **PKCδ promoter activity is stimulated by Sp family members of transcription factors in NIE115 and MN9D cells.** *A*, variable amounts (μg) of pN3-Sp1, pN3-Sp3 FL, pN3-Sp4, or pcDNA-Sp2 expression plasmid or empty vector (pN3 or pcDNA3.1), as indicated, were cotransfected with the PKCδ promoter reporter construct pGL3−147/+289 into NIE115 (*black bar*) and MN9D (*gray bar*) cells. Luciferase activity was measured after 24 h of transfection. The plasmid pcDNA3.1-βgal was included in each transfection for data normalization. Values are expressed as fold induction relative to that obtained from cells transfected with 8 μg of empty vector (*EV*) and represent the mean ± S.E. of three independent experiments performed in triplicate. Variations in the amount of total DNA were compensated with the corresponding empty vector pN3 or pcDNA3.1. *B*, overexpression of Sp factors in transfected NIE115 (*left panel*) and MN9D (*right panel*) cells was determined by immunoblotting analysis. The cells were transfected with Sp expression plasmids in the same manner as *A*. Whole cell lysates were prepared 24 h after transfection and immunoblotted for Sp1, Sp3, Sp4, or β-actin (loading control). Both short Sp3 (sSp3) and long Sp3 (lSp3) isoforms are shown. *C*, expression plasmids pN3-Sp1, pN3-Sp3 FL, pN3-Sp4, and empty vector pN3 were cotransfected along with the PKCδ promoter reporter construct pGL3−147/+289 into NIE115 either alone or in the different combinations, as indicated (μg) *below* the *bar graph*. Luciferase activity was determined after 24 h of transfection. Data shown represent the mean ± S.E. of three independent experiments performed in triplicate.

2.7-fold, which approximates the combined contributions from transfection of individual Sp3 (1.5-fold induction) and Sp1 (1.4-fold induction). These results indicate that the effects of Sp1 and Sp3 are additive to activate expression of the PKCδ promoter. Also, cotransfection of Sp4 with Sp1 or Sp3 (Fig. 4*C*), as well as cotransfection of Sp3 with Sp2 (supplemental Fig. S1), results in a similar additive induction of PKCδ promoter transcription. Thus, the Sp family members exert additive response rather than synergistic or competitive effects on the transcription of the PKCδ promoter in NIE115 cells.

To further clarify the contributions of the different Sp-regulatory elements, including the proximal CACCC box and four distal GC boxes, to the Sp-mediated increase in PKCδ promoter activity in NIE115 cells, we performed site-directed mutagenesis of these sites in the context of the pGL3−147/+209 and pGL3+165/+289 constructs. The former possesses the proximal CACCC site, whereas in the latter only the four GC boxes are present (Fig. 5*A*). The pGL3−147/+209 construct displayed much higher responsiveness to Sp1, Sp3, and Sp4 than did the pGL3+166/+289 construct in transfected NIE115 cells, although a similar level of Sp2-mediated activation was obtained for these two constructs (Fig. 5, *B* and *C*). As expected, mutation of the CACCC site in region −147/+209 (mCACCC) exhibited greatly reduced basal and Sp1-, Sp3-, or Sp4-mediated transcriptional activities relative to the wild-type pGL3−147/+209 construct. Moreover, complete loss of Sp2-mediated activation was observed with the same mutant (Fig. 5*B*). These results indicate that the proximal CACCC element

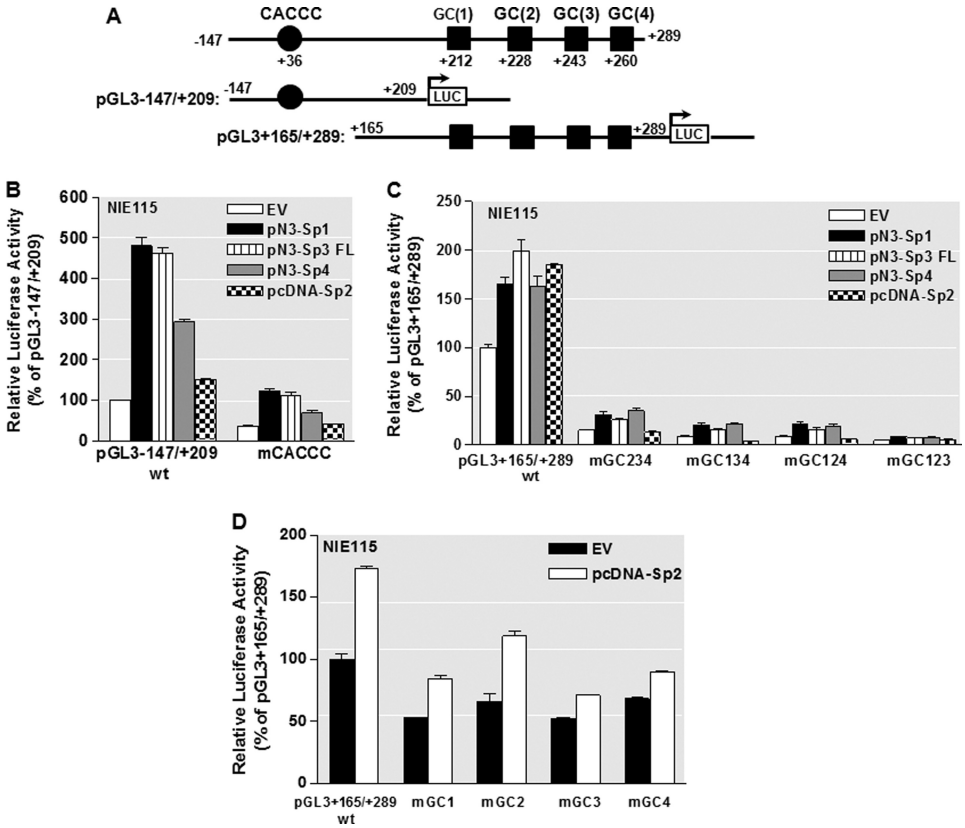

FIGURE 5. **Effects of site-directed mutagenesis of Sp-binding sites on PKCδ promoter activity transactivated by overexpression of Sp transcription factors in NIE115 cells.** NIE115 cells were cotransfected with the indicated wild-type or mutated PKCδ reporter constructs and 8 μg of pN3-Sp1, pN3-Sp3 FL, pN3-Sp4, pcDNA-Sp2, or empty vector (*EV*) pN3 or pcDNA3.1. Luciferase activities were assayed after 24 h. The plasmid pcDNA3.1-βgal was included in each transfection to adjust for transfection efficiency. The activity obtained following cotransfection of the wild-type construct (pGL3−147/+209 or pGL3+165/+289) with empty vector (*EV*) was arbitrarily set to 100, and all other data are expressed as a percentage thereof. The results represent the mean ± S.E. of three independent experiments performed in triplicate. *A*, schematic representation of the wild-type PKCδ promoter reporter constructs pGL3−147/+209 and pGL3+165/+289. The potential Sp sites are depicted by either a *circle* or *square*. *B*, NIE115 cells were cotransfected with 4 μg of either wild-type (pGL3−147/+209) or mCACCC mutated luciferase reporter constructs along with 8 μg of the expression plasmids pN3-Sp1, pN3-Sp3 FL, pN3-Sp4, pcDNA-Sp2, or empty vector (pN3 or pcDNA3.1). *C*, wild-type (pGL3+165/+289) or triple mutated luciferase reporter constructs, as indicated, were cotransfected into NIE115 cells along with the expression plasmids for Sp family members of transcription factors. *D*, wild-type (pGL3+165/+289) or single mutated luciferase reporter constructs, as indicated, were cotransfected into NIE115 cells along with the pcDNA-Sp2 or empty pcDNA3.1 expression vector.

was able to respond to Sp1-, Sp2-, Sp3-, and Sp4-mediated activation of PKCδ promoter. In addition, because the CACCC mutation did not completely abolish the responsiveness to Sp1, Sp3, and Sp4 overexpression, there may be additional GC boxes present in pGL3−147/+209. In the +165/+289 region, similar to previous experiments, triple mutants mGC123, mGC124, mGC134, or mGC134, in which only site GC(4), GC(3), GC(2), or GC(1) is still active, respectively, all resulted in a strong negative effect on basal promoter activity. Somewhat surprisingly, these mutants did not decrease the inducibility of wild-type pGL3+165/+289 by Sp1, Sp3, or Sp4. However, this was not the case of Sp2-mediated activation where these triple mutants abolished all Sp2-mediated transactivation potential. On the other hand, the Sp2 expression vector activated the single mutants mGC(1), mGC(2), mGC(3), or mGC(4) to a similar extent as the wild-type pGL3+165/+289 promoter construct (Fig. 5*D*). These results indicate that each of the four distal GC boxes is sufficient to mediate response to Sp1, Sp3, or Sp4 overexpression, whereas cooperative interactions among the different GC sites are required to mediate the transactivation effect of Sp2 on the PKCδ promoter.

Functional Analysis of the Mouse PKCδ Promoter in Drosophila SL2 Cells—To further address the transcriptional functions displayed by members of the Sp families of transcription factors in regulation of mouse PKCδ gene transcription, *Drosophila* SL2 cells, which are deficient in endogenous Sp-related proteins (52), were utilized. The SL2 cells are devoid of many ubiquitous mammalian transcription factor activities (63, 64); thus, their transcriptional properties can be investigated in the absence of interference by endogenous factors. Varying amounts of expression vectors (1–4 μg) under the control of the insect actin promoter for Sp1 (pPac-Sp1), Sp2 (pPac-Sp2), Sp4 (pPac-Sp4), the long (pPac-USp3) and short isoforms of Sp3 (pPac-Sp3), the full length of Sp3 (pPac-Sp3FL encoding long and short isoforms of Sp3 like the mammalian expression vector pN3-Sp3 FL in Fig. 4), and empty pPac0 vector together with the PKCδ promoter construct pGL3−147/+289 were individually transfected into SL2 cells. The β-galactosidase insect expression vector p97b was included to monitor transfection efficiency. Normalized luciferase activities were compared with those obtained with empty vector pPac0. As shown in Fig. 6*A*, addition of either pPac-Sp1 or pPac-Sp4 slightly

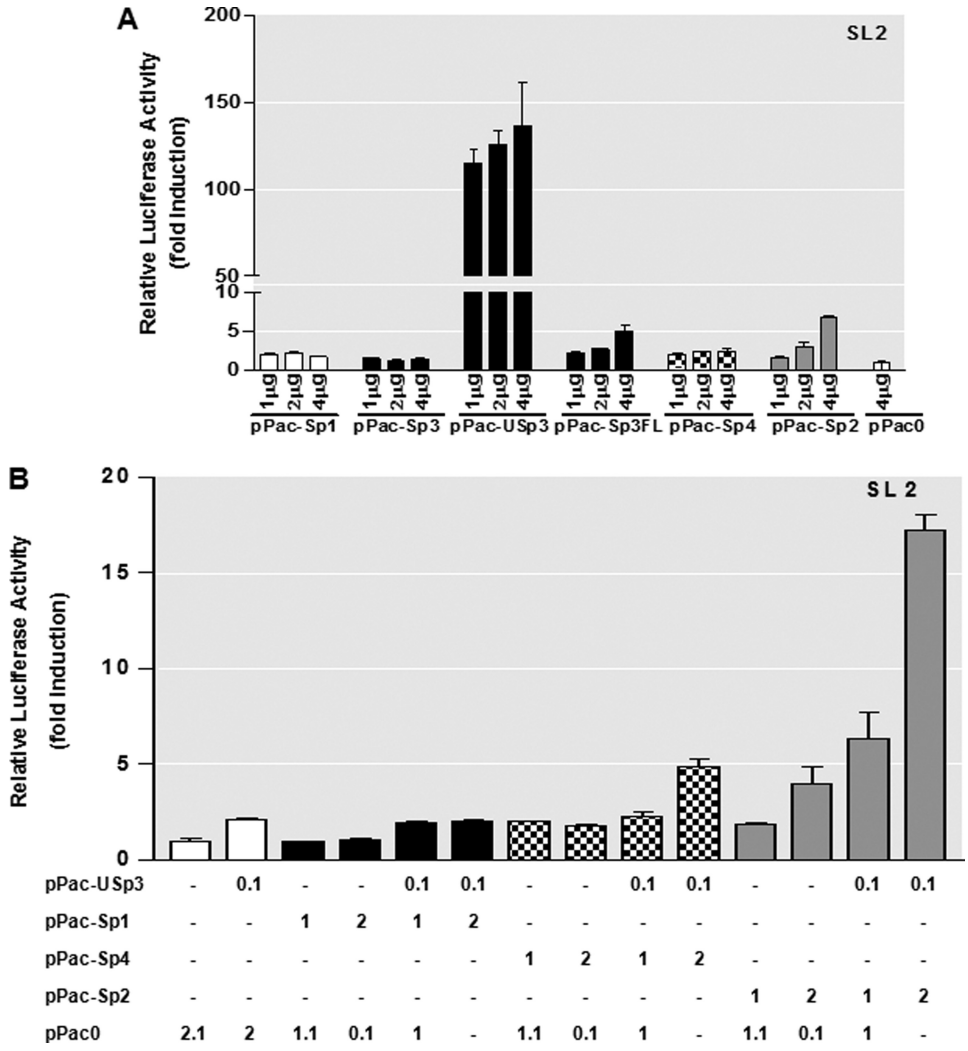

FIGURE 6. **Effects of overexpression of Sp family members of transcription factors on the PKCδ promoter activity in SL2 cells.** *A*, PKCδ promoter reporter construct pGL3−147/+289 (4 μg) was cotransfected with variable amounts (1–4 μg) of *Drosophila* expression plasmids for Sp1 (pPac-Sp1), the short isoform of Sp3 (pPac-Sp3), the long isoform of Sp3 (pPac-USp3), the full length of Sp3 (pPac-Sp3FL), Sp4 (pN3-Sp4), or Sp2 (pPac-Sp2) in *Drosophila* SL2 cells. Luciferase activity was measured after 48 h of transfection. The *Drosophila* β-gal expression plasmid p97b was included in each transfection for data normalization. Values are expressed as fold induction relative to that obtained from cells transfected with 4 μg of empty vector (pPac0) and represent the mean ± S.E. of three independent experiments performed in triplicate. Variations in the amount of total DNA were compensated with the corresponding empty vector pPac0. *B*, *Drosophila* expression plasmids pPac-USp3, pPac-Sp1, pPac-Sp4, and pPac-Sp2 were cotransfected along with 4 μg of PKCδ promoter reporter construct pGL3−147/+289 into SL2 cells either alone or in the different combinations, as indicated (μg) *below* the *bar graph*. Variations in the amount of total DNA were compensated with the corresponding empty vector pPac0. Luciferase activity was determined after 48 h of transfection. Transfection efficiency was normalized by β-galactosidase activity. Values are expressed as fold induction relative to that obtained from cells transfected with pPac0 alone and represent the mean ± S.E. of three independent experiments performed in triplicate.

increased PKCδ promoter activity in a dose-dependent manner. The optimal stimulation (2.3-fold) was saturated at 2 μg of pPac-Sp1 or pPac-Sp4. Interestingly, a dual effect was seen when different isoforms of Sp3 were transfected into SL2 cells. Increasing amounts of the short isoform of Sp3 plasmid (pPac-Sp3) had no effect on transactivation of the PKCδ promoter. In contrast, cotransfection of pGL3−147/+289 with the long isoform of Sp3 plasmid (pPac-USp3) induced a maximal 136.2-fold increase in luciferase activity. In addition, the pGL3−147/+289 promoter activity was also activated in a dose-dependent manner by expression with either pPac-Sp2 or pPac-Sp3FL, reaching maximal 6.9- and 5.0-fold stimulation with 4 μg of pPac-Sp2 or pPac-Sp3FL, respectively. These results indicate that the long isoform of Sp3, but not the short isoform of Sp3, is a potent activator of the PKCδ promoter in *Drosophila* SL2 cells and that Sp1, Sp2, and Sp4 exert weak positive effects on the transactivation of the PKCδ promoter.

Because overexpression of Sp1, Sp2, or Sp4 only modestly increased PKCδ promoter activity in SL2 cells, we next investigated the interplay between them with the long isoform of Sp3 in PKCδ gene regulation. As shown in Fig. 6*B*, cotransfections of varying amounts of pPac-Sp1 (1–2 μg) with a fixed amount of the pPac-USp3 (0.1 μg) had no effect on promoter activation of pGL3−147/+289. Likewise, there was no significant stimulation of luciferase activity when 1 μg of pPac-Sp4 was cotransfected with 0.1 μg of pPac-USp3, and similar to the mammalian expression system, an additive transactivation was seen after cotransfection of 2 μg of pPac-Sp4 with pPac-USp3. In contrast, combining pPac-USp3 with either 1 μg (6.4-fold induction) or 2 μg (17.0-fold

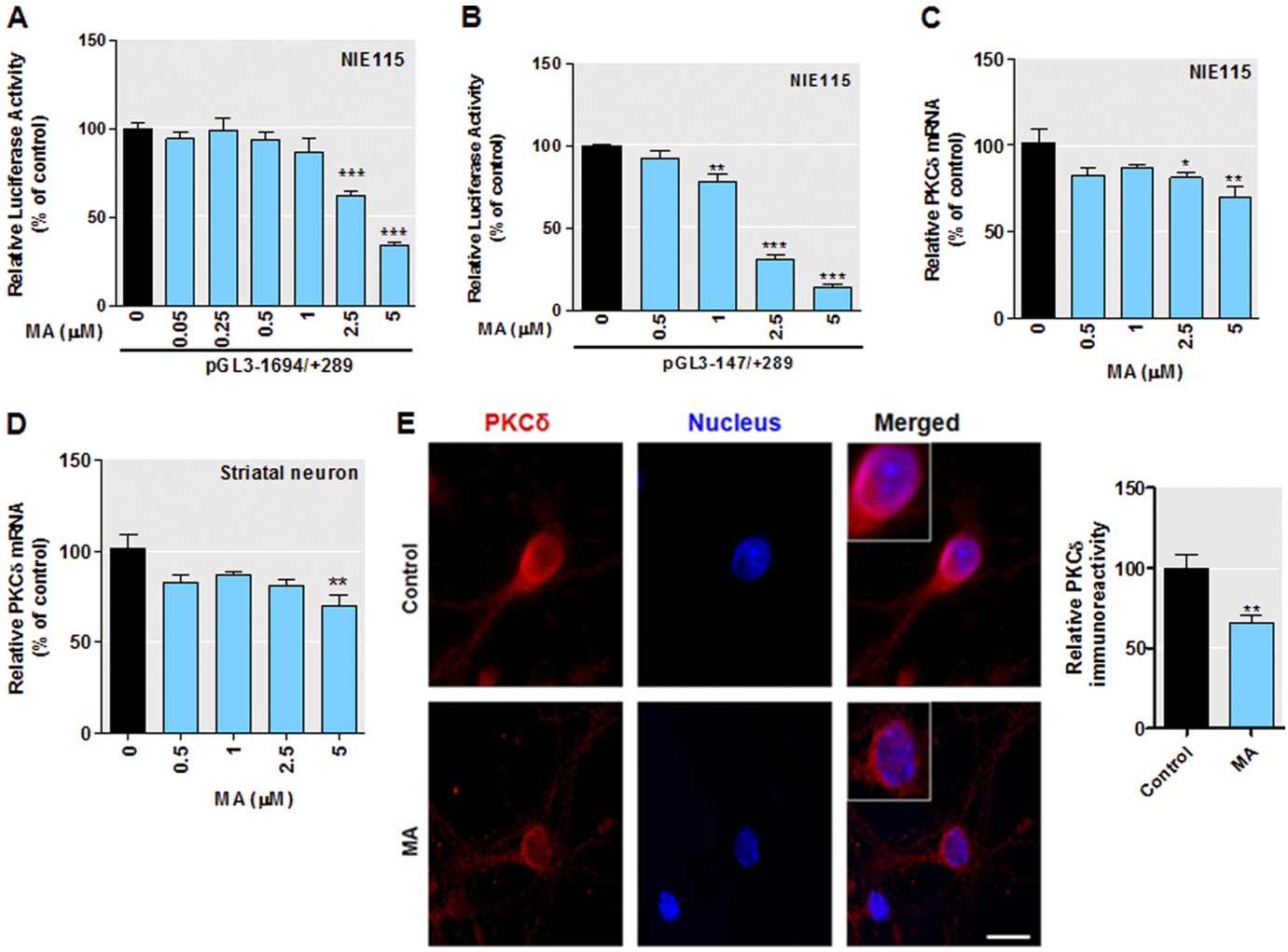

FIGURE 7. **Mithramycin A (*MA*) inhibits expression of the mouse *Prkcd* gene.** *A* and *B*, PKCδ promoter activity is attenuated in NIE115 cells after treatment with mithramycin A. The PKCδ promoter reporter construct pGL3−1694/+289 (*A*) or pGL3−147/+289 (*B*) was transfected into NIE115 cells. After 4 h of transfection, the cells were incubated with or without Sp factor inhibitor mithramycin A at concentrations ranging from 0.05 to 5 μM for 24 h. Cells were then harvested, and luciferase activities were determined. The plasmid pcDNA3.1-βgal was included in each transfection to correct the differences in transfection efficiencies. Values are expressed as a percentage of the activity of control and represent the mean ± S.E. of three independent experiments performed in triplicate. (**, $p < 0.01$; ***, $p < 0.001$; between the control and mithramycin A-treated samples.) *C* and *D*, endogenous PKCδ mRNA levels are reduced by mithramycin A. NIE115 cells (*C*) or primary striatal neurons (*D*) were treated with different concentrations of mithramycin A for 24 h. Real time RT PCR analysis of PKCδ mRNA level was performed. β-Actin mRNA level was served as internal control. Values are expressed as a percentage of the activity of control and represent the mean ± S.E. of three independent experiments performed in triplicate. (*, $p < 0.05$; **, $p < 0.01$ compared with the control and mithramycin A-treated samples.) *E*, *left panel,* exposure of primary striatal neurons to 5 μM mithramycin A reduced PKCδ immunoreactivity. Primary striatal cultures were treated with or without 5 μM MA for 24 h. Cultures were immunostained for PKCδ (*red*), and the nuclei were counterstained by Hoechst 33342 (*blue*). Images were obtained using a Nikon TE2000 fluorescence microscope (magnification ×60). *Scale bar,* 10 μm. Representative immunofluorescence images are shown. The *inset* shows a higher magnification of the cell body area. *Right panel,* immunofluorescence quantification of PKCδ fluorescence intensity. Fluorescence immunoreactivity of PKCδ was measured in each group using Metamorph software. Values expressed as percent of control group are mean ± S.E. and representative for results obtained from three separate experiments in triplicate (**, $p < 0.01$).

induction) of pPac-Sp2 resulted in a synergistic transactivation of PKCδ promoter activity. This is different from the data in mammalian cells (supplemental Fig. S1), indicating that two different mechanisms may be operative in insect and mammalian cells.

Mithramycin A Inhibits PKCδ Gene Expression—To further confirm the role of Sp transcription factors on PKCδ expression, we examined the inhibition of the exogenous PKCδ promoter activity by mithramycin A, which is known to bind to the GC-rich motif and inhibit Sp transcription factor binding (65, 66). The transiently transfected NIE115 cells were treated with increasing doses of mithramycin A, and the effects of mithramycin A on PKCδ promoter activity were analyzed by luciferase assays. The mithramycin A concentrations used were not toxic to NIE115 cells. As shown in Fig. 7, addition of mithramycin A to transfected cells led to a dose-dependent decrease in promoter activity for both reporter construct pGL3−147/+289 (Fig. 7*A*) and full-length pGL3−1694/+289 (Fig. 7*B*). At the highest dose of mithramycin A (5 μM), the transcriptional activity of pGL3−147/+289 and pGL3−1694/+289 was dropped by 60 and 80%, respectively. In addition, we also performed a real time RT-PCR assay to investigate the effects of mithramycin A on the endogenous PKCδ expression in NIE115 cells (Fig. 7*C*). Dose studies indicated that incubation with the highest dose of mithramycin A (5 μM) for 24 h resulted in a modest but significant reduction in PKCδ mRNA expression by ~30%. Further-

more, the inhibition of PKCδ endogenous expression by mithramycin A was confirmed in additional biochemical experiments in primary striatal cell culture. The primary striatal neurons were chose because striatum represents a relatively homogeneous population of interneurons with dopaminergic innervation as compared with the substantia nigra, and thus it offers an amenable model for biochemical analysis. As shown in Fig. 7*D*, similar to the trend seen in the NIE115 cells, the highest dose of mithramycin A (5 μM) induced an ~30% decrease in PKCδ mRNA in primary striatal neurons. Immunocytochemical analysis of PKCδ immunoreactivity of striatal neurons substantiated the inhibitory effect of mithramycin A on PKCδ gene expression (Fig. 7*E*, *left panel*). Quantification of the PKCδ fluorescent intensity with Metamorph Image analysis software revealed an ~35% ($p < 0.01$) reduction in PKCδ immunoreactivity in 5 μM mithramycin A-treated neurons (Fig. 7*E*, *right panel*). Altogether, these results again established that PKCδ expression is Sp factor-dependent. In addition, because the repression of PKCδ transcripts at the endogenous level by mithramycin A (Fig. 7*C*) was far less pronounced than that of the exogenous promoter reporter activity (Fig. 7, *A* and *B*), regulation of the endogenous PKCδ may also be controlled by additional mechanisms that are not manifested in exogenous reporter plasmids during a transient luciferase assay.

Binding of Sp Family of Transcription Factors to the PKCδ Promoter in NIE115 Cells—To directly address whether Sp family proteins are associated with the PKCδ promoter *in vivo*, we performed a chromatin immunoprecipitation assay. NIE115 cells were transfected with either the expression vectors for Sp proteins or the empty vector, and proteins were then formaldehyde cross-linked to chromatin. The immunoprecipitation was performed with antibody directed against Sp1, Sp3, or Sp4. The precipitated DNA was isolated and subjected to PCR analysis with the primer set P+2F/P+289R encompassing the promoter region +2 to +289. In the empty vector control samples, an expected 312-bp DNA fragment was amplified from DNA immunoprecipitated by Sp3 or Sp4 antibody but not from Sp1 immunoprecipitation (Fig. 8*A*, *lanes 2–4*). This result correlates with the previous observation that Sp1 factor is present at extremely low or undetectable levels in NIE115 cells (Fig. 4*B*). Furthermore, significantly increased levels of amplification of the PKCδ promoter were observed in DNA immunoprecipitated by any of the Sp antibodies from Sp-enriched cells when compared with levels seen for empty vector transfected controls (Fig. 8*A*, *lane 2 versus 7*, *lane 3 versus 10*, and *lane 4 versus 13*). Together, the ChIP results provide evidence for direct *in vivo* association of Sp proteins with the PKCδ promoter in the chromatin of NIE115 cells.

For an additional experiment to further characterize the binding of Sp proteins to the PKCδ proximal promoter region, we performed gel shift assays using a double-stranded 32-bp IRye™ 700-labeled oligonucleotide (+205/+236) (see supplemental Table S2 for all oligonucleotides used in EMSA experiments) containing the two proximal Sp-binding sites GC(1) and GC(2) as probe. As shown in Fig. 8*B* (*lane 2*), a shift protein-DNA complex band was detected after incubating the probe with NIE115 nuclear extracts. This shifted band was almost completely abolished either by addition of an excess of the unlabeled +205/+236 self-oligonucleotide or by an Sp1 consensus oligonucleotide, establishing the nucleic acid-protein binding specificity (Fig. 8*B*, *lanes 3* and *5*). In contrast, when a 100-fold molar excess of unlabeled mutant +205/+236 self-oligonucleotide, in which the GC(1) and GC(2) motifs were double mutated (Fig. 8*B*, *lane 4*) or unlabeled mutant Sp1 consensus oligonucleotide (Fig. 8*B*, *lane 6*) was used, the formation of a specific complex was only partially blocked. Moreover, the addition of excess of either an unlabeled PKCδ +218/+238 oligonucleotide or unlabeled PKCδ +201/+220 oligonucleotide corresponding to the single GC(2) or GC(1) motif, respectively (Fig. 8*B*, *lanes 7* and *8*), failed to completely abrogate the formation of the DNA-protein complex, suggesting that GC(1) and GC(2) boxes are both functional binding sites for the DNA-protein interaction of this complex. In addition, another shifted band without competition by excess of the unlabeled +205/+236 oligonucleotide was considered as nonspecific binding and marked as N.S. in Fig. 8*B*.

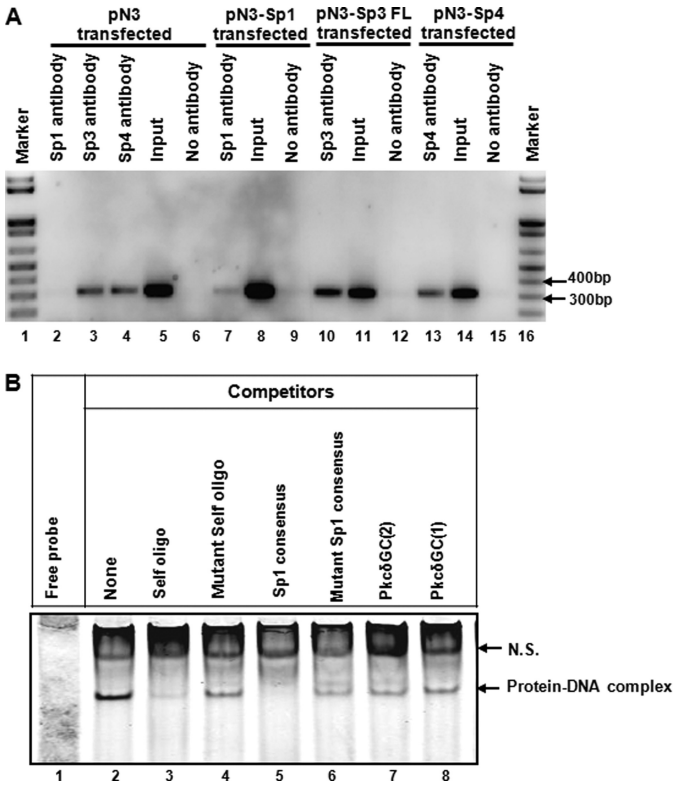

FIGURE 8. **Binding of Sp family of transcription factors to the PKCδ promoter in NIE115 cells.** *A*, ChIP assays in NIE115 cells indicate a physical association of Sp1, Sp3, and Sp4 with the PKCδ promoter region. Cross-linked chromatin was isolated from NIE115 cells transfected with the expression plasmids for Sp1 (pN3-Sp1), Sp3 (pN3-Sp3 FL), Sp4 (pN3-Sp4), or the empty vector pN3, as indicated. Isolated chromatin was enzymatically digested and immunoprecipitated with anti-Sp1 (*lanes 2* and *7*), anti-Sp3 (*lanes 3* and *10*), anti-Sp4 (*lanes 4* and *13*), or antibody-free control (*lanes 6, 9, 12,* and *15*). The subsequently purified DNA from immunoprecipitated samples and unimmunoprecipitated samples (labeled as *Input*, *lanes 5, 8, 11,* and *14*) was subjected to PCR amplification with primers specific for PKCδ promoter region that generates a 312-bp fragment. *B*, EMSA to test binding of nuclear proteins from NIE115 cells with the Sp site of the PKCδ promoter. EMSA was performed with an IRye700-labeled probe corresponding to the PKCδ promoter GC(1) and GC(2) motifs and 10 μg of nuclear extract from NIE115 cells. As indicated, various competitors (100-fold excess of unlabeled oligonucleotides, *lanes 3–8*) were added to the mixture before adding probe. The sequences of the competitors are shown in supplemental Table S2. The specific and nonspecific (labeled as *N.S.*) complexes are indicated by *arrows*.

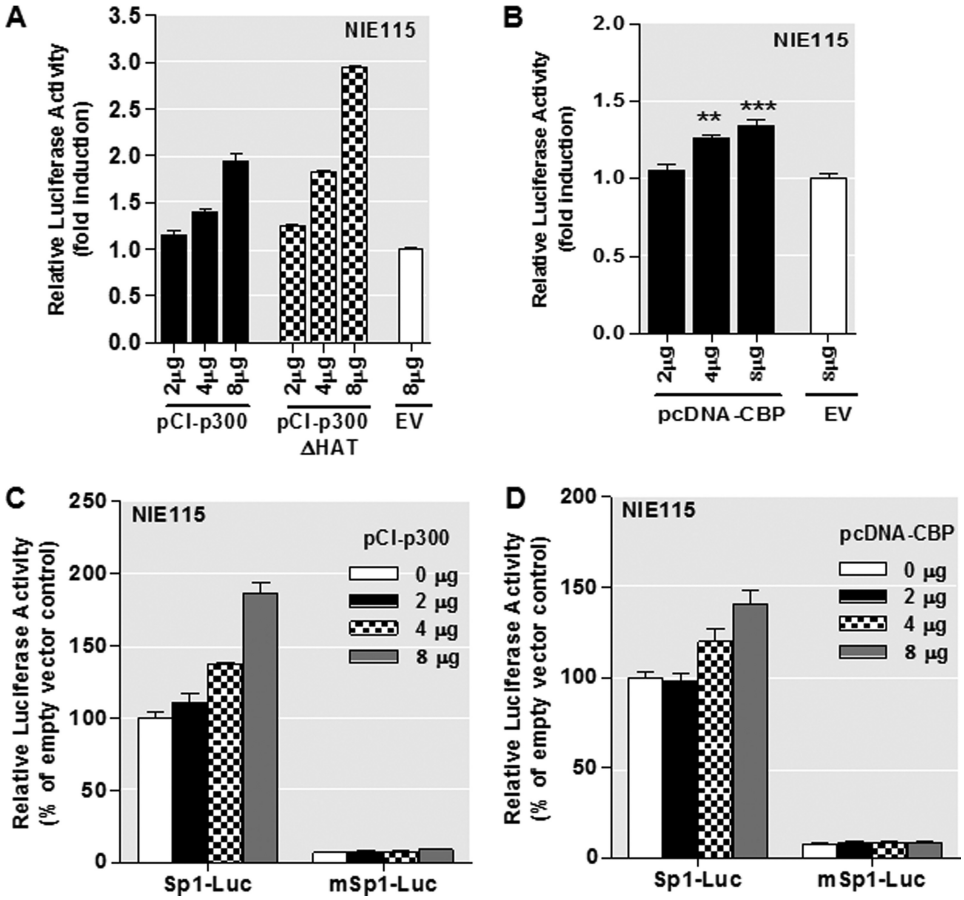

FIGURE 9. **PKCδ promoter activity is stimulated by p300/CBP in NIE115 cells, and this effect is independent of p300 HAT activity and requires functional Sp sites.** *A* and *B*, variable amounts (μg) of expression plasmid for p300 (pCI-p300) and p300 mutant (pCI-p300ΔHAT) (*A*) or CBP (pcDNA-CBP) (*B*) were cotransfected with the PKCδ promoter reporter construct pGL3−147/+289 into NIE115 cells. Variations in the amount of total DNA were compensated with the corresponding empty vector (*EV*) pCIneo or pcDNA3.1. Luciferase activity was measured after 24 h of transfection. The plasmid pcDNA3.1-βgal was included in each transfection for data normalization. Values are expressed as fold induction relative to that obtained from cells transfected with 8 μg of empty vector and represent the mean ± S.E. of three independent experiments performed in triplicate. (**, $p < 0.01$; ***, $p < 0.001$; as compared with the EV-transfected samples.) *C* and *D*, luciferase reporter constructs Sp1-Luc or mSp1-Luc were cotransfected with variable amounts (μg) of expression plasmid pCI-p300 (*C*) or pcDNA-CBP (*D*) were into NIE115 cells. Luciferase activity was measured after 24 h of transfection. Values are expressed as percent of that obtained from cells cotransfected with 8 μg of EV and wild-type Sp1-Luc construct and represent the mean ± S.E. of three independent experiments performed in triplicate.

Coactivators p300/CBP Stimulate PKCδ Promoter Activity through Sp-binding Sites in NIE115 Cells—Because p300/CBP can function as coactivators of Sp transcription factors, we next analyzed whether they play a role in regulating mouse PKCδ gene expression by studying the effect of ectopic p300/CBP expression on promoter activation of the pGL3−147/+289 construct in NIE115 cells. As shown in Fig. 9, *A* and *B*, both p300 and CBP significantly enhance the PKCδ promoter activity. Interestingly, when a mutant p300 protein without intrinsic HAT activity was overexpressed, an even stronger up-regulation of PKCδ promoter activity was seen (Fig. 9*A*), suggesting that the HAT activity of p300 is not required for transactivating the PKCδ promoter. Moreover, to assess whether p300/CBP meditate their transcriptional activation through the Sp sites, two luciferase reporter constructs, Sp1-Luc and mSp1-Luc, which contain three consensus Sp1-binding sites and three mutant Sp1 sites, respectively, were utilized. As shown in Fig. 9, *C* and *D*, similar to the PKCδ promoter construct pGL3−147/+289, overexpression of p300/CBP significantly stimulated the wild-type Sp1-Luc activity, whereas the mutant mSp1-Luc completely lost the responsiveness to increased expression of p300/CBP, suggesting that the stimulatory effect of p300/CBP may be mediated through the Sp-binding sites on the PKCδ promoter.

Ectopic PKCδ Expression Increased Vulnerability of Dopaminergic Neurons to Oxidative Stress-stimulated Degeneration—Oxidative stress, arising due to excessive production of reactive oxygen species and/or defective reactive oxygen species removal has long been implicated in the pathogenesis of many neurodegenerative diseases, including PD (67, 68). Based on our observation that nigral dopaminergic neurons display high levels of PKCδ expression (13) and that proteolytic activation of this kinase plays a key role in meditating oxidative stress-dependent neurodegeneration (7), we further assessed whether the extent of PKCδ expression correlates with H_2O_2-induced degeneration. To address this, we performed ectopic expression of PKCδ in MN9D dopaminergic neurons and investigated its effect on H_2O_2-induced apoptotic cell death. Fluorescence microscopic imaging of PKCδ-GFP-transfected cells revealed that ~60% of cells were expressing PKCδ-GFP proteins (Fig. 10, *right panel*), confirming the high efficiency of ectopic expression of PKCδ in MN9D cells. Quantification of H_2O_2-induced cell death in the EGFP-C1 control vector-transfected cells by

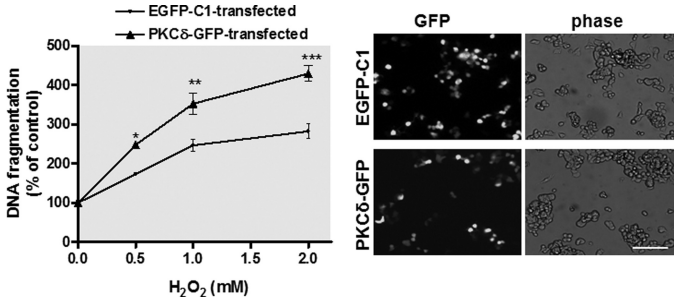

FIGURE 10. **Overexpression of PKCδ sensitizes MN9D dopaminergic cells to oxidative stress-dependent neurodegeneration.** MN9D cells were transfected with plasmid expressing PKCδ-GFP or control plasmid EGFP-C1 for 18 h. The cells were then switched to a serum-free medium and exposed to various doses of H_2O_2, ranging from 0.5 to 2.0 mM for 20 h. Cells were collected and assayed for DNA fragmentation (*left panel*). Data shown represent mean ± S.E. from two independent experiments performed in quadruplicate (*, $p < 0.05$; **, $p < 0.01$; ***, $p < 0.001$; compared with the control and H_2O_2-treated samples). The overexpression of PKCδ-GFP was confirmed by GFP fluorescence imaging (*right panel*). Images were obtained using a Nikon TE2000 fluorescence microscope (magnification ×20). *Black* and *white* GFP fluorescence images were presented. *Scale bar,* 100 μm.

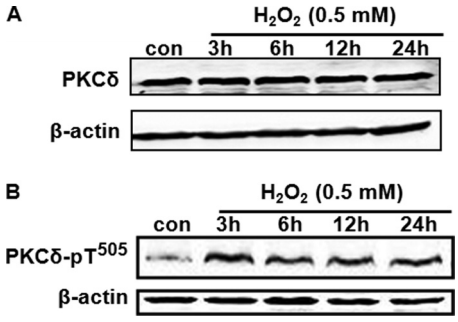

FIGURE 11. **Treatment with H_2O_2 increases Thr^{505} phosphorylation of PKCδ without affecting PKCδ expression.** MN9D cells were incubated with 0.5 mM H_2O_2 for various time spans (3–24 h) and then were harvested for measurement of native PKCδ (*A*) or PKCδ Thr505 phosphorylation (*B*) levels by Western blot analysis. β-Actin was used as a loading control. Representative immunoblots are shown. *con*, control.

DNA fragmentation assay showed that H_2O_2 treatment dose-dependently induced neuronal degeneration, having a maximum (~300% of untreated cells) at dose 2 mM. In contrast, overexpression of PKCδ induced an increased level of H_2O_2-induced DNA fragmentation (Fig. 10, *left panel*). These results suggest that the level of PKCδ gene expression may have important regulatory roles in oxidative stress-dependent neurodegeneration.

Previous studies have identified PKCδ as a key mediator of oxidative damage induced by ischemia/reperfusion (2, 17, 69). Moreover, elevated expression of PKCδ has been observed in brain tissue after cerebral ischemia (14–17). Thus, in this study we investigated whether oxidative stress causes any change in PKCδ gene expression. As shown in Fig. 11*A*, exposure of MN9D cells to 0.5 mM H_2O_2 for up to 24 h did not up-regulate the protein levels of PKCδ. Also, a similar time course study with H_2O_2 treatment (0.5 and 1 mM) did not show a significant induction of PKCδ mRNA levels in MN9D cells, as measured by quantitative RT-PCR analysis (data not shown). Next, we examined whether oxidative stress can induce threonine (Thr^{505}) phosphorylation of PKCδ because phosphorylation of activation loop threonine (Thr^{505}) has been reported to be important for PKCδ activity (70–73). As shown in Fig. 11*B*, treatment with 0.5 mM H_2O_2 significantly increased the phosphorylation of PKCδ Thr^{505}, with a maximal effect at 3–6 h. These observations suggest that acute oxidative stress does not alter the *de novo* synthesis of PKCδ, but rather it induces rapid activation of PKCδ by activation loop phosphorylation.

Inhibition of PKCδ Transcription Ameliorates Oxidative Stress-induced Neurodegeneration—As described above, we have demonstrated that the Sp family of transcription factors, particularly the long Sp3 isoform, induces PKCδ gene activity in neuronal cells and primary neurons via multiple Sp-binding elements and that high levels of PKCδ protein are associated with an exacerbated sensitivity to oxidative stress. To further demonstrate the functional significance of PKCδ transcriptional control by Sp proteins in oxidative stress-dependent neurodegeneration, MN9D dopaminergic cells were pretreated with Sp inhibitor mithramycin A, and then oxidative stress-induced cell death was measured. The cells were pretreated with varying concentrations of Sp inhibitor mithramycin A (1 and 2.5 μM) for 12 h, followed by the exposure of cells to 1 mM H_2O_2. Twelve hours later, cell viability was measured using the SYTOX® Green cytotoxicity assay. As shown in Fig. 12, *A* and *B*, exposure to H_2O_2 led to significantly greater toxicity in MN9D cells. In contrast, pretreatment of MN9D cells with mithramycin A inhibited H_2O_2-induced cytotoxicity. Mithramycin A did not alter basal cell viability. Consistent with the SYTOX® Green viability assay, quantification of caspase-3 enzymatic activities revealed that the pretreatment with mithramycin A also significantly reduced the H_2O_2-induced caspase-3 activation in a dose-dependent manner (Fig. 12*C*). These results demonstrate that controlling PKCδ transcription via inhibition of the activation of Sp proteins can ameliorate the oxidative stress-elicited neuronal cell death, suggesting that Sp proteins may serve as potential therapeutic targets for treatment of oxidative damage in dopaminergic neuronal cells.

In parallel with studies utilizing a pharmacological approach to prevent Sp transactivation, we also used a dominant-negative form of Sp3 that has an intact C-terminal DNA binding domain but lacks the N-terminal full transactivation domains, as described previously (51). We transiently transfected MN9D cells with constructs encoding wild-type Sp3 (pN3-Sp3 FL), dominant-negative Sp3 (pN3-DN-Sp3), or empty vector (pN3), and we then exposed cells to 0.5 mM H_2O_2 for 20 h. These cells were subsequently assayed for cell viability using the SYTOX® Green cytotoxicity assay. As shown in Fig. 12*D*, increasing amounts of the wild-type Sp3 expression plasmid significantly enhanced H_2O_2-induced cell death as compared with the cells transfected with vehicle vector, mirroring our previous results with direct PKCδ overexpression (Fig. 10). In contrast, even the highest amount of the dominant-negative Sp3 had no significant effect on cell viability in the presence of H_2O_2. Taken together, our experiments with mithramycin A and DN-Sp3 strongly suggest that inhibition of PKCδ transcription can protect dopaminergic neuronal cells against oxidative stress-induced cell injury.

DISCUSSION

This study addresses the regulatory *cis*-acting elements and candidate regulatory factors involved in the transcription of the

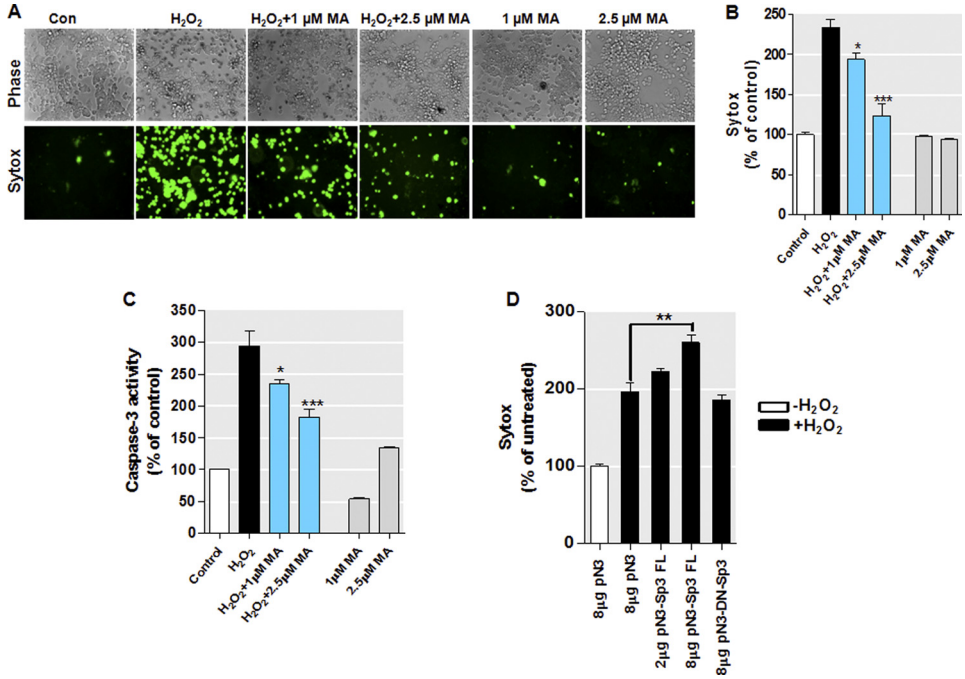

FIGURE 12. **Inhibition of PKCδ transcription ameliorates oxidative stress-induced cell death in a dopaminergic neuronal model.** *A–C*, pretreatment with MA inhibited the oxidative stress response in MN9D dopaminergic cells. The cells were preincubated with varying doses of MA for 12 h before treatment with H_2O_2 (1 mM) and then assayed for cell death (*A* and *B*) and caspase-3 activity (*C*). Cell death was measured using the SYTOX® Green cytotoxicity assay as described under "Experimental Procedures." Representative phase contrast (*top*) and SYTOX® Green staining (*bottom*) images are shown. Images were obtained using a Nikon TE2000 fluorescence microscope (magnification ×20). The caspase-3 activity or cytotoxicity was determined and expressed as a percentage of induction relative to unstimulated controls (*Con*). The results represent the mean ± S.E. of two independent experiments performed in pentaplicate (*, $p < 0.05$; ***, $p < 0.001$; as compared with the samples treated with H_2O_2 alone). *D*, overexpression of dominant-negative mutant Sp3 protein (pN3-DN-Sp3) lacking the transactivation domains did not enhance the H_2O_2-induced cell death in MN9D cells. The cells were transfected with indicated amounts of constructs encoding full-length Sp3 (*pN3-Sp3 FL*), dominant-negative Sp3 (*pN3-DN-Sp3*), or vehicle vector (*pN3*) for 16 h. Cells were then exposed to 0.5 mM H_2O_2 for 20 h, and H_2O_2-induced cell death was determined using the SYTOX® Green cytotoxicity assay. Variations in the amount of total DNA were compensated with the empty vector pN3. The results represent the mean ± S.E. of two independent experiments performed in pentaplicate (**, $p < 0.01$; between the H_2O_2-treated samples that were transfected with pN3 or pN3-Sp3 FL vectors).

mouse *Prkcd* gene in neuronal cells. PKCδ has been widely identified as a pro-apoptotic effector of signals in various cell types (2, 74, 75). Recent evidence supports a prominent role for caspase-dependent PKCδ activation in oxidative stress-induced dopaminergic cell death in experimental models of PD because of a high expression of the kinase in nigrostriatal dopaminergic neurons (5, 6, 13). Despite extensive investigations of the molecular mechanisms of activation of PKCδ, relatively little information is available on the mechanisms that control PKCδ expression at the transcriptional level (42–45). Previous studies on the regulatory elements of the PKCδ gene are all based on analysis of the 5′-flanking sequences upstream of the TSS; however, no attempt was made to examine the importance of the GC-rich domains in the first exon. Emerging evidence indicates that the noncoding region in the exon downstream of TSS has been recognized as a major regulatory region of various gene expressions (48, 77–80). Thus, we cloned and characterized the mouse PKCδ promoter, including the first exon GC-rich sequences, in an effort to define mechanisms underlying the transcriptional regulation of PKCδ.

In this study, an ~2.0-kb fragment of mouse genomic DNA encompassing the 5′-flanking region and the partial first exon of the *Prkcd* gene was isolated and cloned into a luciferase reporter vector. The PKCδ promoter does not have a consensus TATA motif in the vicinity of the TSS (40). Our own sequence analysis found further upstream TATA-like elements at −1651, −1185, and −932 (data not shown). However, these TATA-like motifs appear to be nonfunctional, as no significant transcriptional activity was observed in the region between −1694 and −659 (Fig. 1*B*, pGL3−1694/−659). Additionally, other known core promoter motifs, such as the CAAT box, initiator element, and downstream promoter element, were not identified at consensus positions within the PKCδ promoter.

We showed that the 2.0-kb PKCδ promoter/luciferase construct displayed significant transcriptional activity (Fig. 1*B*, ~30 times higher than the promoterless pGL3-Basic vector) upon transfection into the PKCδ-expressing neuronal cell lines NIE115 and MN9D. Deletion analysis of this 2.0-kb region revealed multiple positive and negative elements, all of which contribute to the PKCδ expression. A strong negative element (NREI) present at −660 to −147 is capable of repressing the gene activity by 100%. Negative elements have also been implicated in the regulation of several other PKC family genes. For example, a silencer-like element at −1821 to −1702 was identified for the human PKCη promoter (81). Furthermore, we characterized that this element is not in itself a true silencer but rather functions as a PKCδ promoter-specific repressive element. Computational analysis of this region did not reveal significant sequence identity with any known silencer motif; however, it contains multiple TFBS (data not shown), such as an overlapping STAT1/Ets site (−656 to −639) and an adjacent NF-Y site (−637 to −627), as well as a downstream WHNF site

(−596 to −591). Notably, STAT1, Ets, and NF-Y are all known to serve a dual role in transcriptional regulation as an activator or as a repressor (82, 83). Whether these elements are involved in the repressing activity has yet to be determined. Studies are underway to dissect the exact location of this negative element and the proteins that bind to it. Additionally, located farther upstream of NREI is another negative regulatory element (NREII, between −1694 and −1193). This element, however, is relatively weak.

In deletion studies we also identified two novel positive regulatory elements within the 2.0-kb region of the PKCδ promoter. We previously identified a basal PKCδ promoter (−147 bp to the TSS) that displays ~6 times greater activity over the pGL3-Basic vector in NIE115 and MN9D cells (Fig. 1*B*, *pGL3−147/+2*) and an NFκB and NERF1a sites are responsible for its activity.[3] In this study, we found that the downstream fragment in exon 1 from bp +2 to +289 was capable of dramatically enhancing the basal PKCδ promoter activity in both NIE115 and MN9D cells (Fig. 1*B*), suggesting that this region contains most of the positive *cis*-acting elements necessary for PKCδ expression. Notably, when the location of this 288-bp positive element was altered, its enhancing activity was entirely lost (Fig. 3*D*). This suggests that proper distance arrangement of this element with respect to the basal PKCδ promoter is important. In addition the region between −147 and +289 appears to confer the greatest transcriptional activity in neurons, thus functioning as a PKCδ core promoter. Of particular interest was an additional positive regulatory element from bp −1192 to −660. This element, which resides directly adjacent to the NREI in the 52-bp region between −712 and −660, was able to significantly overcome the activity of NREI. Curiously, this region acts mechanistically as a novel anti-repressive element. To date, only a few anti-repressive elements have been reported for eukaryotic genes (84). At this time, we could not provide any further characterization of this interesting element or its binding protein. Future studies will address this issue. Taken together from all these studies, the transcription of PKCδ is tightly controlled by multiple elements acting in concert to ensure its differential expression pattern in a variety of biological processes.

Next, the major positive regulatory element immediately downstream of the PKCδ transcription start site (bp from +2 to +289) was analyzed in detail. *In silico* analysis identified four GC boxes in close proximity to each other at +208/+216, +225/+233, +239/+247, and +256/+264, as well as an upstream CACCC box (also called the GT box) at +35/+43 (Fig. 3*A*). The functional importance of these multiple Sp-binding motifs was assessed by site-specific mutagenesis and transfection of the mutated constructs into NIE115 and MN9D cells (Fig. 3*B*). The results showed that all these motifs are functional in activating PKCδ transcription and that the five Sp-binding sites appear functionally different. The magnitude of activating effects is in the order GC(1) or GC(2) > GC(3) > GC(4) or CACCC. Furthermore, an essential role for the cooperative action of all these Sp sites for the transactivation of PKCδ transcription was confirmed. In addition to the Sp-binding sites, i*n silico* analysis also revealed the presence of multiple other TFBS within this +2/+289 segment (data not shown). Conceivably, these *cis*-elements may also contribute to the regulation of PKCδ expression.

The Sp family of transcription factors including Sp1, Sp2, Sp3, and Sp4 are all structurally similar and are the most well characterized GC-rich motif-binding proteins. To elucidate the roles of Sp family members in transcriptional regulation of PKCδ, cotransfection studies using a reporter containing the PKCδ promoter −147/+289 along with Sp expression vectors were performed (Fig. 4*A*). These studies revealed a similar activation profile of Sp transcription factors in NIE115 and MN9D cells, although less pronounced transcriptional activation was observed in the latter. In both cell lines, Sp3 is the strongest transactivator, whereas overexpression of Sp1, Sp2, and Sp4 displayed much less activation of the PKCδ promoter. It should be noted that both NIE115 and MN9D cells expressed easily detectable levels of endogenous Sp3 and Sp4 but undetectable levels of endogenous Sp1(Fig. 4*B*), suggesting that Sp3 and Sp4 may be responsible for a major part of PKCδ promoter activity in these two neuronal cell lines. The contribution of the multiple Sp-binding sites found within the PKCδ promoter to the Sp-mediated promoter activity was further assessed using substitution mutant constructs. By using a smaller construct, namely pGL3−147/+209, which possesses the upstream CACCC motif but lacks the downstream four GC boxes, we found that the CACCC motif is required for complete Sp2-mediated promoter activity in this promoter context (−147 to +209). In contrast, this site is insufficient for complete Sp1, Sp3, and Sp4 transactivation (Fig. 5*B*). This suggests additional Sp-like binding sites within this region that are important for Sp transactivation of the PKCδ promoter. However, cotransfection of Sp expression plasmids with pGL3+165/+289 triple mutant constructs confirmed that each of the four downstream GC boxes is sufficient for complete Sp1, Sp3 and Sp4 transactivation. However, cooperative action of different GC boxes is required for mediating Sp2 transactivation, because triple GC box mutations failed to mediate any Sp2 transactivation (Fig. 5, *C* and *D*). This different mode of action between Sp2 and other Sp family members is not surprising, as they have different DNA binding specificity and affinities. For example, Sp1, Sp3, and Sp4 bind GC boxes with similar specificity and affinities, whereas Sp2 binds with much lower affinity (85).

To analyze precisely the transcriptional roles of the Sp family of transcription factors in a Sp-deficient background, transfection assays were carried out in *Drosophila* SL2 cells (Fig. 6). We demonstrated a dual function of Sp3 in regulating PKCδ transcription; the long isoforms of Sp3 most potently activate the PKCδ promoter, whereas the short isoforms of Sp3 are transcriptionally inactive on their own, which may be due to the absence of the N-terminal transactivation A domain present in the long isoforms of Sp3 (46). These data together suggest that the Sp3 isoform expression may have a dramatic effect on PKCδ expression. Indeed, alteration of the Sp3 isoform ratio has been observed under certain conditions (46). In combination experiments (Fig. 6*B*), overexpression of Sp1 had no effect on the transcriptional activation by the long Sp3 isoform, although

[3] H. Jin, A. Kanthasamy, D. Zhang, V. Anantharam, and A. G. Kanthasamy, unpublished data.

Sp4 was able to transactivate the promoter activation by the long Sp3 isoform in an additive manner, only when a higher amount of Sp4 expression vector was transfected. In contrast, obvious synergistic activation of PKCδ promoter transcription was observed when combining Sp2 with a long isoform of Sp3. However, this finding is not seen in mammalian cells, probably because there is already enough endogenous Sp2 and Sp3 in these cells.

Several additional lines of evidence solidify the essential role of Sp family transcription factors in controlling PKCδ expression. First, by using the Sp inhibitor mithramycin A, we demonstrated that transcription of the PKCδ promoter is dependent on Sp activity (Fig. 7, *A* and *B*). At the highest dose of 5 μM mithramycin A, more than an 80% decrease of full-length PKCδ promoter activity was achieved in NIE115 cells. Second, and more importantly, mithramycin A also suppresses, albeit to a much lesser extent, the endogenous PKCδ expression in NIE115 cells and primary striatal neurons (Fig. 7, *C–E*). This information also suggests that the endogenous *Prkcd* gene is under different layers of regulatory control in addition to the 5′-promoter in the context of an exogenous reporter plasmid. Epigenetic regulatory mechanisms, such as DNA methylation or histone modifications, might be involved in the regulation of PKCδ expression and could account for this complexity. The mouse PKCδ promoter is GC-rich and contains a putative CpG island that is partly methylated in NIE115 and MN9D cells (data not shown). Furthermore, treatment of NIE115 cells by the methylation-specific inhibitor 5′-aza-2′-deoxycytidine significantly increased the endogenous PKCδ mRNA expression and attenuated its methylation status (supplemental Fig. S2). DNA methylation has been shown to interfere with the binding of Sp1 to DNA (86). Experiments are in progress to elucidate whether CpG methylation of the PKCδ promoter could affect the function of Sp transcriptional factors in regulation of PKCδ expression. Third, chromatin immunoprecipitation assays confirmed that transcription factors Sp1, Sp3. and Sp4 bind to the PKCδ promoter for transcriptional activation in NIE115 cells, in the environment of chromatin *in vivo* (Fig. 8*A*). Finally, gel mobility shift assays with nuclear extracts from NIE115 cells detected the formation of one specific complex with the PKCδ +205/+236 oligonucleotide, and the relevance to Sp factors was further confirmed by using specific competitors (Fig. 8*B*).

The Sp factors regulate a variety of genes that are involved in the apoptotic cascade. This has been reported for the caspase-3 (87), caspase-8 (88), FasL (89), and finally as shown in this study for PKCδ. Although the Sp1 factor functions as an activator of transcription, the function of Sp3 is less clear. It is generally accepted that Sp3 is the only protein in the Sp subfamily that can either positively or negatively modulate the gene expression. The role of Sp3 as an activator or repressor remains elusive. Evidence suggests that its activity strongly depends on the structure and arrangement of Sp recognition sites as well as the cell type-specific difference (46). Our results suggest that for the mouse PKCδ basal promoter, Sp3 acts as a strong activator. In addition, regulation of Sp1 and Sp3 activity is achieved by post-translational modifications. For examples, the post-translational modification to Sp1/Sp3 by acetylation stimulates their activity (90, 91), whereas sumoylation of Sp1/Sp3 causes their inactivation (92). Although our Sp1 or Sp3 acetylation immunoprecipitation and Western blot analysis failed to detect any endogenous acetylation of Sp1 or Sp3 in normal NIE115 cells (data not shown), we could not exclude the possibility that Sp1 or Sp3 is acetylated in response to specific stimuli, such as oxidative stress (93). In addition to post-translational modifications, regulation of the activities of Sp family members also includes protein-protein interactions. For example, Sp1 and Sp3 bind directly to p300 and its homolog CBP (94, 95). We previously demonstrated that rat *Prkcd* gene expression is p300-dependent and that p300 associates endogenously with the rat *Prkcd* gene. Nevertheless, the roles of p300/CBP in the facilitation of PKCδ gene expression are still poorly understood. In this study, our evidence suggests that forced expression of p300 or CBP resulted in a dose-dependent activation of mouse PKCδ promoter (Fig. 9, *A* and *B*) in the NIE115 cells. Furthermore, it appears that the GC boxes are crucial for the p300/CBP activation, as overexpression of CBP/p300 did not activate the Sp1-reporter containing mutations in the GC boxes (Fig. 9, *C* and *D*). More interestingly, our results also indicate that p300 may activate PKCδ transcription by HAT-independent mechanisms (Fig. 9*A*), which may partly explain why we could not detect any endogenous acetylation of Sp1 or Sp3 in NIE115 cells.

In addition to the mechanism of alterations in PKCδ gene expression, the kinase activity can be modulated by multiple integrated mechanisms. These include caspase-mediated proteolysis, coordinated phosphorylation, and dynamic regulation of its subcellular distribution (3, 74). Considering the complexity of the mechanisms of PKCδ regulation and the fact that PKCδ is significantly involved in numerous cellular functions, PKCδ signaling must be tightly controlled. In fact, deregulation of the PKCδ pathway has been implicated in several disease conditions. For example, altered expression of PKCδ has been shown to be associated with the progression of malignant tumors (18–28). Increasing evidence also suggests a role for PKCδ in the development of stroke reperfusion injury (17). Using gene knock-out studies, it has been shown that mice deficient in PKCδ exhibit a striking 70% reduction in stroke size during reperfusion, as compared with wild-type littermates (96). Pharmacological inhibition of PKCδ by peptide inhibitor also caused a similar effect (97). Elevated protein and mRNA expression of PKCδ in ischemic brain tissue of rats further strengthens the support for the role of PKCδ in ischemia/reperfusion injuries (14). Furthermore, PKC signaling represents a key element of the molecular changes associated with aging (98–100). Although it appears that PKC isoform levels were not affected in rat cortex during brain aging (98, 101, 102), impaired activity of PKCδ as well as other novel PKC isoforms has been reported (98, 99). An age-associated increase in expression and activation of PKCδ in the aged heart has been demonstrated in a number of studies (103, 104). These observations confirm that the functional properties of PKCδ can vary depending on the biological context, such as the cell type, the tissue, and the developmental stage (2, 3). Notably, PKCδ is an oxidative stress-sensitive kinase that can be activated by various oxidative insults (2, 3, 7, 105, 106). Consistent with this notion, our results demonstrate that acute exposure of MN9D dop-

aminergic neurons to hydrogen peroxide results in a rapid activation of the kinase by active loop phosphorylation (Fig. 11*B*). Although PKCδ expression was not altered by acute exposure of hydrogen peroxide (Fig. 11*A*), prolonged exposure might cause the induction of this protein. Recently, we have provided evidence that PKCδ serves as a key modulator of stress-induced dopaminergic neurodegeneration (5–7, 10, 36, 76). Intraperitoneal injection or oral administration of the PKCδ inhibitor significantly protected nigral dopaminergic neurons in a 1-methyl-4-phenyl-1,2,3,6-tetrahydropyridine-induced animal model of Parkinson disease (11). In this study, we found that the expression of PKCδ is closely linked to the oxidative stress-induced neurodegeneration (Fig. 10), which raises the intriguing possibility of development of new drugs targeting the kinase. Importantly, blockade of PKCδ transactivation by the Sp factor inhibitor, mithramycin A, successfully protected MN9D dopaminergic neurons from oxidative stress-induced neuronal injury (Fig. 12).

In summary, we have functionally characterized for the first time, the regulation of the PKCδ gene promoter. Our results clearly indicate that multiple positive and negative regulatory elements contribute to PKCδ promoter expression. In particular, we have identified the core promoter located between nucleotides −147 and +289, and we demonstrated a functional role for five Sp sites within this region in the regulation of constitutive PKCδ expression. We have also shown that Sp1, Sp3, and Sp4 directly bind to the PKCδ promoter through the multiple Sp sites and positively regulate PKCδ expression. Furthermore, ectopic expression studies revealed that the expression level of the PKCδ gene correlates well with the sensitization of dopamine neurons to oxidative stress-induced neuronal cell death (Fig. 10). Importantly, our findings also emphasize the functional importance of PKCδ transcriptional control designed to inhibit the expression and/or function of PKCδ via blockade of Sp-dependent transactivation in regulating oxidative stress-induced apoptotic response in dopaminergic neurons (Fig. 12). Taken together with our previous observation that PKCδ plays a critical role in the oxidative stress-induced dopaminergic degeneration in PD (7, 10) and that PKCδ inhibition has been explored in preclinical models of PD (11, 12), these findings have important implications for the utility of PKCδ as a target in developing novel drug therapies against oxidative damage in PD.

Acknowledgment—We thank Mary Ann deVries for assistance in the preparation of this manuscript.

REFERENCES

1. Dempsey, E. C., Newton, A. C., Mochly-Rosen, D., Fields, A. P., Reyland, M. E., Insel, P. A., and Messing, R. O. (2000) *Am. J. Physiol. Lung Cell. Mol. Physiol.* **279,** L429–L438
2. Brodie, C., and Blumberg, P. M. (2003) *Apoptosis* **8,** 19–27
3. Steinberg, S. F. (2004) *Biochem. J.* **384,** 449–459
4. Saito, N. (1995) *Nippon Yakurigaku Zasshi* **105,** 127–136
5. Anantharam, V., Kitazawa, M., Wagner, J., Kaul, S., and Kanthasamy, A. G. (2002) *J. Neurosci.* **22,** 1738–1751
6. Kaul, S., Kanthasamy, A., Kitazawa, M., Anantharam, V., and Kanthasamy, A. G. (2003) *Eur. J. Neurosci.* **18,** 1387–1401
7. Kaul, S., Anantharam, V., Yang, Y., Choi, C. J., Kanthasamy, A., and Kanthasamy, A. G. (2005) *J. Biol. Chem.* **280,** 28721–28730
8. Kitazawa, M., Anantharam, V., and Kanthasamy, A. G. (2003) *Neuroscience* **119,** 945–964
9. Latchoumycandane, C., Anantharam, V., Kitazawa, M., Yang, Y., Kanthasamy, A., and Kanthasamy, A. G. (2005) *J. Pharmacol. Exp. Ther.* **313,** 46–55
10. Yang, Y., Kaul, S., Zhang, D., Anantharam, V., and Kanthasamy, A. G. (2004) *Mol. Cell. Neurosci.* **25,** 406–421
11. Zhang, D., Anantharam, V., Kanthasamy, A., and Kanthasamy, A. G. (2007) *J. Pharmacol. Exp. Ther.* **322,** 913–922
12. Kanthasamy, A. G., Anantharam, V., Zhang, D., Latchoumycandane, C., Jin, H., Kaul, S., and Kanthasamy, A. (2006) *Free Radic. Biol. Med.* **41,** 1578–1589
13. Zhang, D., Kanthasamy, A., Yang, Y., Anantharam, V., and Kanthasamy, A. (2007) *J. Neurosci.* **27,** 5349–5362
14. Miettinen, S., Roivainen, R., Keinänen, R., Hökfelt, T., and Koistinaho, J. (1996) *J. Neurosci.* **16,** 6236–6245
15. Li, X., Ma, C., Zhu, D., Meng, L., Guo, L., Wang, Y., Zhang, L., Li, Z., and Li, E. (2010) *Prostaglandins Other Lipid Mediat.* **93,** 84–92
16. Hlaváčková, M., Kožichová, K., Neckář, J., Kolář, F., Musters, R. J., Novák, F., and Nováková, O. (2010) *Mol. Cell. Biochem.* **345,** 271–282
17. Chou, W. H., and Messing, R. O. (2005) *Trends Cardiovasc. Med.* **15,** 47–51
18. Vucenik, I., Ramakrishna, G., Tantivejkul, K., Anderson, L. M., and Ramljak, D. (2005) *Breast Cancer Res. Treat.* **91,** 35–45
19. Reno, E. M., Haughian, J. M., Dimitrova, I. K., Jackson, T. A., Shroyer, K. R., and Bradford, A. P. (2008) *Hum. Pathol.* **39,** 21–29
20. Alonso-Escolano, D., Medina, C., Cieslik, K., Radomski, A., Jurasz, P., Santos-Martínez, M. J., Jiffar, T., Ruvolo, P., and Radomski, M. W. (2006) *J. Pharmacol. Exp. Ther.* **318,** 373–380
21. Kharait, S., Dhir, R., Lauffenburger, D., and Wells, A. (2006) *Biochem. Biophys. Res. Commun.* **343,** 848–856
22. Villar, J., Arenas, M. I., MacCarthy, C. M., Blánquez, M. J., Tirado, O. M., and Notario, V. (2007) *Cancer Res.* **67,** 10859–10868
23. Kiley, S. C., Clark, K. J., Duddy, S. K., Welch, D. R., and Jaken, S. (1999) *Oncogene* **18,** 6748–6757
24. Kruger, J. S., and Reddy, K. B. (2003) *Mol. Cancer Res.* **1,** 801–809
25. Evans, J. D., Cornford, P. A., Dodson, A., Neoptolemos, J. P., and Foster, C. S. (2003) *Am. J. Clin. Pathol.* **119,** 392–402
26. Koike, K., Fujii, T., Nakamura, A. M., Yokoyama, G., Yamana, H., Kuwano, M., and Shirouzu, K. (2006) *Thyroid* **16,** 333–341
27. Balasubramanian, N., Advani, S. H., and Zingde, S. M. (2002) *Leuk. Res.* **26,** 67–81
28. Tsai, J. H., Hsieh, Y. S., Kuo, S. J., Chen, S. T., Yu, S. Y., Huang, C. Y., Chang, A. C., Wang, Y. W., Tsai, M. T., and Liu, J. Y. (2000) *Cancer Lett.* **161,** 171–175
29. Ono, Y., Fujii, T., Ogita, K., Kikkawa, U., Igarashi, K., and Nishizuka, Y. (1988) *J. Biol. Chem.* **263,** 6927–6932
30. Leibersperger, H., Gschwendt, M., Gernold, M., and Marks, F. (1991) *J. Biol. Chem.* **266,** 14778–14784
31. Naik, M. U., Benedikz, E., Hernandez, I., Libien, J., Hrabe, J., Valsamis, M., Dow-Edwards, D., Osman, M., and Sacktor, T. C. (2000) *J. Comp. Neurol.* **426,** 243–258
32. Barmack, N. H., Qian, Z., and Yoshimura, J. (2000) *J. Comp. Neurol.* **427,** 235–254
33. Shanmugam, M., Krett, N. L., Maizels, E. T., Cutler, R. E., Jr., Peters, C. A., Smith, L. M., O'Brien, M. L., Park-Sarge, O. K., Rosen, S. T., and Hunzicker-Dunn, M. (1999) *Mol. Cell. Endocrinol.* **148,** 109–118
34. Peters, C. A., Cutler, R. E., Maizels, E. T., Robertson, M. C., Shiu, R. P., Fields, P., and Hunzicker-Dunn, M. (2000) *Mol. Cell. Endocrinol.* **162,** 181–191
35. Berry, D. M., Antochi, R., Bhatia, M., and Meckling-Gill, K. A. (1996) *J. Biol. Chem.* **271,** 16090–16096
36. Kanthasamy, A. G., Kitazawa, M., Kaul, S., Yang, Y., Lahiri, D. K., Anantharam, V., and Kanthasamy, A. (2003) *Ann. N.Y. Acad. Sci.* **1010,** 683–686
37. Shin, S. Y., Kim, C. G., Ko, J., Min, D. S., Chang, J. S., Ohba, M., Kuroki, T., Choi, Y. B., Kim, Y. H., Na, D. S., Kim, J. W., and Lee, Y. H. (2004) *J. Mol.*

Biol. **340,** 681–693
38. Choi, S. H., Hyman, T., and Blumberg, P. M. (2006) *Cancer Res.* **66,** 7261–7269
39. Horovitz-Fried, M., Cooper, D. R., Patel, N. A., Cipok, M., Brand, C., Bak, A., Inbar, A., Jacob, A. I., and Sampson, S. R. (2006) *Cell. Signal.* **18,** 183–193
40. Suh, K. S., Tatunchak, T. T., Crutchley, J. M., Edwards, L. E., Marin, K. G., and Yuspa, S. H. (2003) *Genomics* **82,** 57–67
41. Kurkinen, K. M., Keinänen, R. A., Karhu, R., and Koistinaho, J. (2000) *Gene* **242,** 115–123
42. Liu, J., Yang, D., Minemoto, Y., Leitges, M., Rosner, M. R., and Lin, A. (2006) *Mol. Cell* **21,** 467–480
43. Horovitz-Fried, M., Jacob, A. I., Cooper, D. R., and Sampson, S. R. (2007) *Cell. Signal.* **19,** 556–562
44. Gavrielides, M. V., Gonzalez-Guerrico, A. M., Riobo, N. A., and Kazanietz, M. G. (2006) *Cancer Res.* **66,** 11792–11801
45. Ponassi, R., Terrinoni, A., Chikh, A., Rufini, A., Lena, A. M., Sayan, B. S., Melino, G., and Candi, E. (2006) *Biochem. Pharmacol.* **72,** 1417–1422
46. Sapetschnig, A., Koch, F., Rischitor, G., Mennenga, T., and Suske, G. (2004) *J. Biol. Chem.* **279,** 42095–42105
47. López-Soto, A., Quiñones-Lombraña, A., López-Arbesú, R., López-Larrea, C., and González, S. (2006) *J. Biol. Chem.* **281,** 30419–30430
48. Saur, D., Seidler, B., Paehge, H., Schusdziarra, V., and Allescher, H. D. (2002) *J. Biol. Chem.* **277,** 25798–25814
49. Boyes, J., Byfield, P., Nakatani, Y., and Ogryzko, V. (1998) *Nature* **396,** 594–598
50. Yang, X. J., Ogryzko, V. V., Nishikawa, J., Howard, B. H., and Nakatani, Y. (1996) *Nature* **382,** 319–324
51. Sowa, Y., Orita, T., Minamikawa-Hiranabe, S., Mizuno, T., Nomura, H., and Sakai, T. (1999) *Cancer Res.* **59,** 4266–4270
52. Suske, G. (2000) *Methods Mol. Biol.* **130,** 175–187
53. Livak, K. J., and Schmittgen, T. D. (2001) *Methods* **25,** 402–408
54. Tavares, D., Tully, K., and Dobner, P. R. (1999) *J. Biol. Chem.* **274,** 30066–30079
55. Roth, B. L., Poot, M., Yue, S. T., and Millard, P. J. (1997) *Appl. Environ. Microbiol.* **63,** 2421–2431
56. Sherer, T. B., Betarbet, R., Stout, A. K., Lund, S., Baptista, M., Panov, A. V., Cookson, M. R., and Greenamyre, J. T. (2002) *J. Neurosci.* **22,** 7006–7015
57. Kaul, S., Anantharam, V., Kanthasamy, A., and Kanthasamy, A. G. (2005) *Brain Res. Mol. Brain Res.* **139,** 137–152
58. Morgenstern, B., Dress, A., and Werner, T. (1996) *Proc. Natl. Acad. Sci. U.S.A.* **93,** 12098–12103
59. Cartharius, K., Frech, K., Grote, K., Klocke, B., Haltmeier, M., Klingenhoff, A., Frisch, M., Bayerlein, M., and Werner, T. (2005) *Bioinformatics* **21,** 2933–2942
60. Brand, A. H., Breeden, L., Abraham, J., Sternglanz, R., and Nasmyth, K. (1985) *Cell* **41,** 41–48
61. Black, A. R., Black, J. D., and Azizkhan-Clifford, J. (2001) *J. Cell. Physiol.* **188,** 143–160
62. Suske, G. (1999) *Gene* **238,** 291–300
63. Courey, A. J., and Tjian, R. (1988) *Cell* **55,** 887–898
64. Noti, J. D. (1997) *J. Biol. Chem.* **272,** 24038–24045
65. Ray, R., Snyder, R. C., Thomas, S., Koller, C. A., and Miller, D. M. (1989) *J. Clin. Invest.* **83,** 2003–2007
66. Blume, S. W., Snyder, R. C., Ray, R., Thomas, S., Koller, C. A., and Miller, D. M. (1991) *J. Clin. Invest.* **88,** 1613–1621
67. Greenamyre, J. T., and Hastings, T. G. (2004) *Science* **304,** 1120–1122
68. Jenner, P. (2003) *Ann. Neurol.* **53,** S26–S38
69. Majumder, P. K., Mishra, N. C., Sun, X., Bharti, A., Kharbanda, S., Saxena, S., and Kufe, D. (2001) *Cell Growth Differ.* **12,** 465–470
70. Le Good, J. A., Ziegler, W. H., Parekh, D. B., Alessi, D. R., Cohen, P., and Parker, P. J. (1998) *Science* **281,** 2042–2045
71. Rybin, V. O., Guo, J., Gertsberg, Z., Elouardighi, H., and Steinberg, S. F. (2007) *J. Biol. Chem.* **282,** 23631–23638
72. Welman, A., Griffiths, J. R., Whetton, A. D., and Dive, C. (2007) *Protein Sci.* **16,** 2711–2715
73. Stempka, L., Schnölzer, M., Radke, S., Rincke, G., Marks, F., and Gschwendt, M. (1999) *J. Biol. Chem.* **274,** 8886–8892
74. Kanthasamy, A. G., Kitazawa, M., Kanthasamy, A., and Anantharam, V. (2003) *Antioxid. Redox. Signal.* **5,** 609–620
75. DeVries, T. A., Neville, M. C., and Reyland, M. E. (2002) *EMBO J.* **21,** 6050–6060
76. Kanthasamy, A., Jin, H., Mehrotra, S., Mishra, R., Kanthasamy, A., and Rana, A. (2010) *Neurotoxicology* **31,** 555–561
77. Karban, A. S., Okazaki, T., Panhuysen, C. I., Gallegos, T., Potter, J. J., Bailey-Wilson, J. E., Silverberg, M. S., Duerr, R. H., Cho, J. H., Gregersen, P. K., Wu, Y., Achkar, J. P., Dassopoulos, T., Mezey, E., Bayless, T. M., Nouvet, F. J., and Brant, S. R. (2004) *Hum. Mol. Genet.* **13,** 35–45
78. MacCarthy-Morrogh, L., Wood, L., Brimmell, M., Johnson, P. W., and Packham, G. (2000) *Oncogene* **19,** 5534–5538
79. Whetstine, J. R., Flatley, R. M., and Matherly, L. H. (2002) *Biochem. J.* **367,** 629–640
80. Solovyev, V. V., and Shahmuradov, I. A. (2003) *Nucleic Acids Res.* **31,** 3540–3545
81. Quan, T., and Fisher, G. J. (1999) *J. Biol. Chem.* **274,** 28566–28574
82. Mavrothalassitis, G., and Ghysdael, J. (2000) *Oncogene* **19,** 6524–6532
83. Ramana, C. V., Chatterjee-Kishore, M., Nguyen, H., and Stark, G. R. (2000) *Oncogene* **19,** 2619–2627
84. Wu, Y., Diab, I., Zhang, X., Izmailova, E. S., and Zehner, Z. E. (2004) *Oncogene* **23,** 168–178
85. Hagen, G., Müller, S., Beato, M., and Suske, G. (1992) *Nucleic Acids Res.* **20,** 5519–5525
86. Kudo, S. (1998) *Mol. Cell. Biol.* **18,** 5492–5499
87. Sudhakar, C., Jain, N., and Swarup, G. (2008) *FEBS J.* **275,** 2200–2213
88. Liedtke, C., Groger, N., Manns, M. P., and Trautwein, C. (2003) *J. Biol. Chem.* **278,** 27593–27604
89. Kavurma, M. M., Santiago, F. S., Bonfoco, E., and Khachigian, L. M. (2001) *J. Biol. Chem.* **276,** 4964–4971
90. Ammanamanchi, S., Freeman, J. W., and Brattain, M. G. (2003) *J. Biol. Chem.* **278,** 35775–35780
91. Hung, J. J., Wang, Y. T., and Chang, W. C. (2006) *Mol. Cell. Biol.* **26,** 1770–1785
92. Spengler, M. L., and Brattain, M. G. (2006) *J. Biol. Chem.* **281,** 5567–5574
93. Ryu, H., Lee, J., Olofsson, B. A., Mwidau, A., Dedeoglu, A., Escudero, M., Flemington, E., Azizkhan-Clifford, J., Ferrante, R. J., Ratan, R. R., and Deodoglu, A. (2003) *Proc. Natl. Acad. Sci. U.S.A.* **100,** 4281–4286
94. Suzuki, T., Kimura, A., Nagai, R., and Horikoshi, M. (2000) *Genes Cells* **5,** 29–41
95. Walker, G. E., Wilson, E. M., Powell, D., and Oh, Y. (2001) *Endocrinology* **142,** 3817–3827
96. Chou, W. H., Choi, D. S., Zhang, H., Mu, D., McMahon, T., Kharazia, V. N., Lowell, C. A., Ferriero, D. M., and Messing, R. O. (2004) *J. Clin. Invest.* **114,** 49–56
97. Bright, R., Raval, A. P., Dembner, J. M., Pérez-Pinzón, M. A., Steinberg, G. K., Yenari, M. A., and Mochly-Rosen, D. (2004) *J. Neurosci.* **24,** 6880–6888
98. Battaini, F., and Pascale, A. (2005) *Ann. N.Y. Acad. Sci.* **1057,** 177–192
99. Pascale, A., Amadio, M., Govoni, S., and Battaini, F. (2007) *Pharmacol. Res.* **55,** 560–569
100. Giorgi, C., Agnoletto, C., Baldini, C., Bononi, A., Bonora, M., Marchi, S., Missiroli, S., Patergnani, S., Poletti, F., Rimessi, A., Zavan, B., and Pinton, P. (2010) *Antioxid. Redox. Signal.* **13,** 1051–1085
101. Battaini, F., Elkabes, S., Bergamaschi, S., Ladisa, V., Lucchi, L., De Graan, P. N., Schuurman, T., Wetsel, W. C., Trabucchi, M., and Govoni, S. (1995) *Neurobiol. Aging* **16,** 137–148
102. Pascale, A., Govoni, S., and Battaini, F. (1998) *Mol. Neurobiol.* **16,** 49–62
103. Cataldi, A., Zingariello, M., Rapino, M., Zara, S., Daniele, F., Di Giulio, C., and Antonucci, A. (2009) *Anat. Rec.* **292,** 1135–1142
104. Takayama, M., Ebihara, Y., and Tani, M. (2001) *Jpn. Circ. J.* **65,** 1071–1076
105. Kaneki, M., Kharbanda, S., Pandey, P., Yoshida, K., Takekawa, M., Liou, J. R., Stone, R., and Kufe, D. (1999) *Mol. Cell. Biol.* **19,** 461–470
106. Sun, X., Wu, F., Datta, R., Kharbanda, S., and Kufe, D. (2000) *J. Biol. Chem.* **275,** 7470–7473